Research Square

Preprints are preliminary reports that have not undergone peer review.
They should not be considered conclusive, used to inform clinical practice,
or referenced by the media as validated information.

T cell receptor γδ is a critical, real-time determinant of unique tissue surveillance mechanisms

Nicolas Veland
The Francis Crick Institute
Bethania Garcia-Cassani
The Francis Crick Institute
Ángela Zarco-Cuadrillero
Department of Immunology, Ophthalmology and Ear, Nose and Throat, Complutense University School of Medicine and 12 de Octubre Health Research Institute, Madrid, Spain
Annamaria Mavrigiannaki
The Francis Crick Institute
Duncan McKenzie
The Francis Crick Institute
Jannik Franken
The Francis Crick Institute https://orcid.org/0009-0006-2460-2841
Ana V Marin
Hospital 12 de Octubre https://orcid.org/0000-0002-7541-3729
Anett Jandke
Department of Biomedicine, University Hospital Basel.
Rosa Andres-ejarque
Centre for Inflammation Biology and Cancer Immunology, King's College London
Adrian Hayday
The Francis Crick Institute
Miguel Munoz-Ruiz
Miguel.Munoz-Ruiz@crick.ac.uk

Department of Immunology, Ophthalmology and Ear, Nose and Throat, Complutense University School of Medicine and 12 de Octubre Health Research Institute, Madrid, Spain

---

Biological Sciences - Article

Keywords:

Posted Date: June 24th, 2025

DOI: https://doi.org/10.21203/rs.3.rs-6803702/v1

License: This work is licensed under a Creative Commons Attribution 4.0 International License.
Read Full License

Additional Declarations:
Yes there is potential Competing Interest. N.V. is currently employed on a sponsored research agreement with Takeda Pharmaceuticals. A.H. receives laboratory research funding from Takeda Pharmaceuticals (starting in February 2023). The remaining authors declare no competing interests.

Resource availability

Lead contact

Further information and requests for resources and reagents should be directed to and will be fulfilled by the lead contacts (A.C.H. & M.M.R.).

Materials availability

Mouse lines generated in this study will be maintained in the lead authors' (A.C.H.'s and M.M.R.'s) current institute's animal house and/or stored locally as frozen embryos and can be made available on request.

Data and code availability

Raw and processed data for the mouse RNA-sequencing (RNA-seq) and Assay for Transposase-Accessible Chromatin using sequencing (ATAC-seq) data generated in this paper are available at NCBI's Gene Expression Omnibus (GEO) repository under the accession identifiers GSE277902 and GSE277903 respectively. Human RNA-seq data generated in this paper is available at GEO repository under the accession identifier GSE297713.

T cell receptor γδ is a critical, real-time determinant of unique tissue surveillance mechanisms

Veland, N.[1, 2], Garcia-Cassani, B.[3,4], Zarco-Cuadrillero A.[4], Mavrigiannaki, A.M.[2], McKenzie, D.R.[2], Franken, J.[2], Marin, A.V.[4], Jandke, A.[5], Andrés-Ejarque, R.[6], Hayday, A.C.[1,2,6,7], and Muñoz-Ruiz, M.[2,4,7]

[1]Peter Gorer Department of Immunobiology, King's College London.
[2]Immunosurveillance Laboratory, The Francis Crick Institute, London, NW11AT, United Kingdom.
[3]Development and Homeostasis of the Nervous System Laboratory, The Francis Crick Institute, London, United Kingdom.
[4]Department of Immunology, Ophthalmology and Ear, Nose and Throat, Complutense University School of Medicine and 12 de Octubre Health Research Institute (imas12), Madrid, Spain.
[5]Departement Biomedizin DBM Hebelstrasse - FG Hess Hebelstrasse 20 4031 Basel, Switzerland.
[6]Centre for Inflammation Biology and Cancer Immunology, King's College London, SE19RT, United Kingdom at King's College London and City of London Cancer Centre, London, United Kingdom.
[7]These authors contributed equally to this study.
Address correspondence to: [mimuruiz@ucm.es][adrian.hayday@kcl.ac.uk]

Abstract

γδ T cells are mediators of immunosurveillance used in the clinic. However, their status remains paradoxical. While many display overt traits of adaptive immunity, several major γδ cell subsets including those in barrier tissues make rapid, seemingly TCR-independent responses phenocopying innate lymphoid cells (ILC). While such uncertainty exists, the requirements for γδ T cell-mediated immunosurveillance will remain unclear. This study resolves the paradox, showing that tissue-intrinsic γδ T cells share an absolute real-time dependence on the TCR for their phenotypes, including so-called innate responses to tissue stress and carcinogenesis. While different tissue-intrinsic γδ subsets showed distinct TCR-dependencies, we identified a shared set of TCR-regulated molecules that was likewise disrupted by acute TCR ablation in human γδ T cells. These findings unequivocally distinguish γδ cells from ILC and establish that immunosurveillance by γδ T cells requires an environment conducive to TCR signalling. [139]

Introduction

As efforts intensify to broaden the reach of immunotherapy, much interest is focused on human γδ T cells, particularly those expressing the Vδ1 chain of the T cell receptor (TCR) which are highly enriched in extralymphoid tissues where many solid tumours form or metastasise[1-3]. Indeed, frequencies and activation states of local Vδ1$^+$ cells are associated with favourable patient outcomes in breast, lung, renal, colorectal and ovarian cancers[4-8]. Vδ1 T cells commonly manifest adaptive immunity, as reflected in durable clonal expansions of cells with highly diverse

TCRs[9,10], recognising native conformations of self-encoded surface proteins overexpressed or mis-expressed by infected or transformed cells[3,11]. Indeed, Vδ1$^+$ T cells are now in clinical trials, with much interest in their TCR specificities[3].

Nonetheless, whether γδ T cell-mediated immunosurveillance has any generalisable real-time requirement for TCRγδ ligands or any other form of TCRγδ signalling is conspicuously unresolved. Specifically, several prominent γδ subsets, including those intrinsically associated with tissues, manifest innate immunity, rapidly responding non-clonally to infections or non-microbial perturbations *via* activation of cytokine and Natural Killer receptors (NKRs)[12-16]. Moreover, responding tumour-associated Vδ1 cells in breast cancers showed no evidence for clonal expansions[4]. Elucidating whether such cells have any ongoing requirement for TCRγδ activity is clearly critical for understanding natural immunosurveillance and for its therapeutic exploitation, e.g., inferring from biopsies whether pathologies are probable γδ targets.

More evidence that γδ cells are *de facto* innate, akin to NK cells and other ILC, is provided by mouse studies showing that prototypic immunopathologies are driven primarily by tissue-intrinsic interleukin-17 (IL-17)-producing γδ T cells responding to IL-1β + IL-23 released within damaged tissues[17,18]. Likewise, there are many examples of innate, nonclonal γδ T cell responses in the settings of inflammation, infection, and cancer[19]. In confronting this paradox, one perspective posits that TCRγδ is mostly required for the cells' development. Thus, Vγ-specific T cell compartments are selected by tissue-specific, epithelial, butyrophilin-like (BTNL) molecules, including Skint1+Skint2 (select mouse epidermal Vγ5$^+$ cells), Btnl1+Btnl6 (select mouse intestinal Vγ7$^+$ cells), and BTNL3+BTNL8 (select human intestinal Vγ4$^+$ cells)[20-23], whereupon the cells may respond innately. The significance of these mechanisms is inferred from genetic associations of *BTNL3/8* variants with increased Crohn's Disease pathology and childhood susceptibility to MIS-C[23,24]. Steady-state targeting of tissue-restricted Btnls evidently induced alterations in local γδ T cell phenotypes[20,25], but this notwithstanding, no generalisable dependencies on TCRγδ have been established.

Compounding this point is the lack of any identified BTNL-regulators for several large, sub-epithelial tissue-intrinsic γδ T cell compartments, e.g., human dermal Vδ1$^+$ cells, and murine Vγ6$^+$ and Vγ4$^+$ cells which exist in many tissues and for which strong TCR engagement has been

considered to anatognise the cells' development[26]. What role if any does TCRγδ fulfil for these reportedly innate cells?

This study resolves these issues. The findings unequivocally demonstrate real-time requirements for TCRγδ to maintain core features of γδ cell phenotypes across different anatomical sites and across species, and to permit γδ T cell responses to tissue damage and carcinogenesis, even in cases hitherto considered as wholly innate. This real-time TCR-dependence clearly distinguishes γδ T cells from NK cells and other ILC, and it sets criteria for γδ T cell surveillance of cancers and other forms of tissue dysregulation.

Results:

Specifically targeting mouse tissue-intrinsic γδ T cells

Murine tissue-intrinsic γδ T cells comprise prominent compartments including epidermal TCRVγ5$^+$ cells; intestinal intraepithelial TCRVγ7$^+$ cells, and subepithelial TCRVγ6$^+$ and TCRVγ4$^+$ cells in many sites including skin, uterus, gingiva, lung, gut and meninges[27,28]. Since TCR-Cγ1 (*Trgc1*) is utilised by all such cells, its acute deletion offered a means to assess any generalisable importance of sustained TCRγδ expression, following the cells' development and tissue localisation (Fig 1a). Efficient TCR-Cγ1 gene segment deletion will truncate VJγ transcripts initiating at the Vγ4/5/6/7 promoters and/or will permit them to be spliced to the downstream Cγ3 gene segment (Fig 1b), which is predicted to be a pseudogene[29], and hence should serve as a biologically neutral marker of gene deletion. By contrast, most systemic γδ T cells express TCR Vγ1-Cγ4 (Fig 1b) and so will be unaffected, thereby limiting potential secondary effects caused by acute loss of γδ T cell competence *in vivo*.

To first establish the practicality and specificity of targeting tissue-intrinsic γδ T cells, we generated a mouse strain, *Trgc1*^{indel}, carrying an internal deletion in *Trgc1*. With the development of Vγ5$^+$ or Vγ6$^+$ thymocytes having ceased perinatally, most γδ T thymocytes in adult mice mature into Vγ4-Cγ1$^+$ and Vγ1-Cγ4$^+$ T cells. By contrast, *Trgc1*^{indel} ("TCR Cγ1 KO") mice harboured essentially no Vγ4-Cγ1$^+$ cells whereas Vγ1-Cγ4$^+$ T cells were present, often in slightly higher numbers, as if to partially compensate (Supp Fig 1a, b). Likewise, Vγ1-Cγ4$^+$ T cells comprised >90% of γδ cells in the spleens and mesenteric lymph nodes of TCR Cγ1 KO mice (Supp Fig 1c), the residual cells likely expressing Vγ2-Cγ2 that is ordinarily expressed by a minority of lymphoid γδ T cells[30]. Importantly, Vγ7$^+$ and Vγ4$^+$ intestinal IEL were essentially ablated in Cγ1 KO mice, partly replaced by Vγ1-Cγ4$^+$ cells and αβ T cells, while canonical Vγ5$^+$ dendritic epidermal T cells (DETC) were mostly replaced by CD3$^+$TCRδ^{neg} cells (Supp Fig 1d), consistent with αβ T cells replacing DETC in TCRδ$^{-/-}$ mice[31]. Having thus established the fidelity of targeting *Trgc1*, we proceeded to inducibly delete it in mature γδ T cell compartments, so as to assess its real-time importance.

Survival of inducibly targeted tissue-intrinsic γδ cells

A floxed allele, TCR-Cγ^{fl}, was engineered (Fig 1a) and the resultant TCR-C$\gamma1^{fl/fl}$ mice crossed to strains expressing a tamoxifen-dependent Cre recombinase controlled by either the TCRδ promoter, to achieve $\gamma\delta$ T cell-specific deletion, or the Rosa26 promoter, to increase the penetrance of deleting *Trgc1* in the gut (note, the Cγ1 gene-segment has no function beyond $\gamma\delta$ T cells and hence its widespread acute deletion should be innocuous). In typical experiments, gene deletion was induced by tamoxifen administration over 7 consecutive days, followed by 7 days to permit complete protein loss from most gene-deleted cells prior to phenotyping (Supp Fig 1e).

For five reasons phenotypic analyses focussed on the epidermis, dermis, and intestinal epithelium. First, Vγ5-C$\gamma1^+$ DETC and intestinal Vγ7-C$\gamma1^+$ IEL represent two distinct compartments developmentally shaped by tissue-specific, TCR Vγ-specific Btnl proteins. Second, V$\gamma7^+$ IEL biology is conserved in humans by BTNL-dependent V$\gamma4^+$ IEL. Third, the two skin compartments contrast greatly in their phenotypes and development since DETC are Btnl-dependent and IFNγ-skewed[22], whereas dermal Vγ4-C$\gamma1^+$ and Vγ6-C$\gamma1^+$ cells have no known selecting elements and are IL-17-skewed. Fourth, established challenges exist for eliciting rapid, non-clonal, innate responses of dermal and epidermal $\gamma\delta$ T cells. Fifth, since epidermal and dermal $\gamma\delta$ T cells cannot be reconstituted in adult mice, any impact on them is not obscured by cell turnover.

To assess the impact of acute Cγ1 deletion, we needed first to exclude that Cre recombinase was leaky in mice not exposed to tamoxifen. This was confirmed for epidermis by showing that TCR$\gamma\delta^+$ cells in unmanipulated TCR$\delta^{CreERT2+/-}$C$\gamma1^{fl/fl}$ mice expressed high levels of CD45 (a signature of DETC) and occurred in comparable frequencies to TCR$\gamma\delta^+$ DETC in TCR$\delta^{CreERT2-/-}$ C$\gamma1^{+/+}$ littermates that carry a w.t. *Trgc1* gene (Supp Fig 1f). With this established, we compared mice in which Cγ1 was inducibly deleted, termed $\gamma\delta^X$, with control "non-deletor" TCR$\gamma\delta$-competent animals, termed $\gamma\delta^{TCR}$, which were variably either tamoxifen-treated C$\gamma1^{fl/fl}$ mice lacking Cre recombinase, or tamoxifen-treated C$\gamma1^{+/+}$ mice harbouring Cre recombinase.

Befitting their name, DETC visualised by confocal microscopy of whole-mount skin preparations appear as highly dendritic cells comprising a large fraction of CD45^{hi} cells in $\gamma\delta^{TCR}$ mice (Fig 1c, upper; note CD45^{dull} cells which can be visualised in adjacent epidermal strata are primarily Langerhans cells). By comparison, TCR$\gamma\delta^+$ cells were rare or absent from $\gamma\delta^X$ mice but there

remained a large population of somewhat less dendritic CD45^{hi} cells (Fig 1c, lower). This rounding is reminiscent of activated DETC[12], and of DETC in mice where Skint1 was transiently blockaded by antibodies[25].

High cell-surface CD3 expression reflects stabilised complexes with TCR chains; thus, surface CD3 levels are low in thymocytes of recombinase-activating gene (RAG)-deficient mice, in which no TCR chains can be assembled[32]. Likewise, although CD45^{hi} cells of $\gamma\delta^{X}$ mice were predominantly TCR$\gamma\delta^{neg}$, CD3 was detected by confocal microscopy on cells that also appeared more rounded than TCR$\gamma\delta^{+}$ DETC, and intracellular CD3 (iCD3) was detected by flow cytometry (Fig 1d). Invariable CD3 expression argues against the large viable population of CD45^{hi}TCR$\gamma\delta^{neg}$ cells (that appeared within one week) in $\gamma\delta^{X}$ mice being NK cells, ILC or B cells, and their failure to express TCRβ excludes their being $\alpha\beta$ T cells (Fig 1d; see also below). Thus, this population comprises DETC that were TCR$\gamma\delta^{+}$ as recently as 7-14 days prior to phenotyping. Intriguingly, these TCR^{neg}CD3^{lo} cells expressed CD103, a TGFβ-regulated marker of many tissue-resident T cells, to discernibly higher levels than control $\gamma\delta^{TCR}$ DETC (Fig 1e), a point considered further below.

Although *Trgc1* deletion was very efficient in $\gamma\delta^{x}$ mice, surface TCR$\gamma\delta$ expression was still detectable on some cells (e.g., Fig 1e), in one case up to ~15% (see Fig 1g, below). Nonetheless, when $\gamma\delta^{X}$ epidermal cells were isolated and exposed *in vitro* to cell-activating antibodies against CD3, TCR downregulation occurred but no functional response, specifically upregulation of the high-affinity IL-2 receptor (CD25) that is critical for sustaining T cell activation (Fig 1f). *En passant*, this functional ablation of the epidermal T cell response contrasts with the capacity of anti-CD3 to promote maturation of CD3^{lo} thymocytes in RAG-deficient mice[32].

To compare TCR$\gamma\delta^{+}$ DETC in $\gamma\delta^{TCR}$ mice and TCR-ablated counterparts in $\gamma\delta^{X}$ mice, we tracked CD45^{hi} cells that failed to stain in a "dump channel" comprising antibodies for TCRβ, MHC Class II (detects Langerhans cells), F4/80 (detects macrophages), and CD19 (detects B cells) (Fig 1g). Again, some residual TCR$\gamma\delta^{+}$ cells were observed in $\gamma\delta^{X}$ mice, but they commonly expressed lower levels of TCR$\gamma\delta$ (Supp Fig 1g), were <2% TCRβ^{+}, and were frequently detectable by anti-Vγ5 and by 17D1, an antibody specific at steady-state for the DETC TCR Vγ5-Vδ1 (Supp Fig 1h; note these data are distinct from those shown in Fig 1g that derive from use of a different antibody): thus, these TCR$\gamma\delta^{+}$ cells are seemingly in transit from w.t. DETC to a TCR-deleted

state. Indeed, Vγ5-Cγ1 transcripts were scarcely detectable in $\gamma\delta^{X}$ epidermis, whereas Vγ5-Cγ3 transcripts were detectable *de novo* (Supp Fig 1i), as was anticpated. Despite a slight downward trend, there was no significant difference in the numbers of $CD45^{+}Dump^{neg}$ cells in $\gamma\delta^{TCR}$ and $\gamma\delta^{X}$ mice for up to two months after one week of tamoxifen treatment (Fig 1g).

In sum, following inducible Cγ1 deletion, most epidermal γδ T cells swiftly lost all detectable TCR protein, with a small fraction seemingly *en route* to that status; there was negligible functional response to TCR engagement, and yet there was no overt impact on cell survival, at least over several weeks. To better characterise those TCR-ablated cells, we developed an additional means to identify them by using mTmG mice in which cells that activate Cre-recombinase shift from $Tomato^{+}$ to gfp^{+}. To assess the reliability of this approach, we examined mice homozygous for *Rosa26.mTmG* and *Trcg1*$^{+/+}$ and carrying one allele of $TCR\delta^{CreERT}$. Prior to tamoxifen-treatment, no gfp^{+} lymphocytes were detectable in the epidermis (Supp Fig 1j), whereas following tamoxifen-treatment, >90% of epidermal $\gamma\delta TCR^{+}$ cells had converted to gfp^{+}, beginning within one week and extending for at least one month later (Supp Fig 1k), re-emphasising high penetrance of $TCR\delta^{creERT2}$ in skin. Demonstrating the fidelity of the $TCR\delta^{creERT2}$ system, >99% of gfp^{+} cells were $TCR\delta^{+}$ with none of the remaining 1% of gfp^{+} cells expressing NK1.1 (that marks NK cells) and only 10% of them expressing TCRβ (i.e., <0.1% of total gfp^{+} cells) (Supp Fig 1l). As expected, $TCR\gamma\delta^{+}gfp^{+}$ cells were $CD45^{hi}$ (Supp Fig 1l).

Having established high penetrance and specificity of the system, we examined *Rosa26.mTmG Trcg1*$^{fl/fl}$ *TCRδ*^{CreER} mice for up to 4 weeks post-tamoxifen treatment. There was a substantial population of evenly distributed $CD45^{hi}$ cells, comparable to w.t. DETC, but they were essentially all TCR-ablated (Supp Fig 1m), gfp^{+} (Fig 1h, Supp Fig 1m), and mostly rounded (Supp Fig 1n), phenocopying a few spontaneously activated DETC detectable in $\gamma\delta^{TCR}$ skin (Fig 1h; Supp Fig 1n). Classified by live-dead staining, $\gamma\delta^{X}$ epidermal gfp^{+} cells showed comparable viability to TCR^{+} gfp^{+} cells from $\gamma\delta^{TCR}$ mice (Supp Fig 1o), and when the cells were purified, their status was confirmed by a complete absence of Vγ5-Cγ1 transcripts (Supp Fig 1p).

Importantly, mTmG mice also allowed us to assess the fate of dermal γδ cells following acute TCR deletion. Initially examining *Rosa26.mTmG Trgc1*$^{+/+}$ *TCRδ*^{CreERT} mice, >80% of $TCR\gamma\delta^{+}$ cells converted to gfp^{+} following tamoxifen treatment (Supp Fig 1q). When $\gamma\delta^{X}$ mTmG mice were then examined, they displayed comparable populations of $CD45^{hi}gfp^{+}$ cells to $\gamma\delta^{TCR}$ mTmG mice

but they were TCRδ^{neg} (Supp fig 1r; upper right), expressed negligible Vγ4-Cγ1 or Vγ6-Cγ1 mRNAs, and were largely viable (Supp Fig 1s,t). Following pre- and perinatal maturation, dermal $\gamma\delta$ cell numbers generally decline slightly over time, as was evident for the frequency of TCR$^+$gfp$^+$ cells among total dermal cells in $\gamma\delta^{TCR}$ mTmG mice over a five-week period post-tamoxifen (Fig 1i). Strikingly, the representation of gfp$^+$TCR^{neg} cells in $\gamma\delta^X$ mTmG mice was completely comparable (Fig 1i). Thus, as in the epidermis, highly penetrant, acute conversion from a TCR$^+$ $\gamma\delta$ cell state to a TCR^{neg} state had negligible impact on the maintenance of the dermal $\gamma\delta$ cell compartment at least over several weeks. Of note, unlike systems in which diptheria toxin is used to inducibly deplete cell popluations, any phenotypic changes in the skin of $\gamma\delta^X$ mice cannot be attributed to a sudden wave of cell death.

Core phenotypic changes following TCR$\gamma\delta$ deletion

The next question was whether the phenotypes of epidermal and dermal $\gamma\delta$ T cells, which are almost completely divergent (see above), would be comparably affected by acute TCR deletion. Thus, we composed an antibody panel focussed on cell-surface proteins collectively considered as key regulators of tissue-resident T cells, and adopted spectral flow cytometry because it can swiftly determine at the single-cell level whether populations segregate from each other for multiple markers. For epidermis, this was conducted on "dump channel negative" cells and for dermis, on gfp$^+$ cells from $\gamma\delta^X$ mice compared to gfp^{neg} cells from w.t. mice.

As expected, epidermal and dermal cells from control mice were heterogeneous, distributing into different clusters, but, additionally, epidermal and dermal cells from $\gamma\delta^X$ mice largely segregated into clusters distinct from their TCR$\gamma\delta^+$ counterparts, even when excluding staining for TCR, CD3, CD45, gfp, and live/dead (Fig 2a-d). Thus, acute TCR deletion had a significant impact on the cells' phenotypes. The clustering was validated *a posteriori* by surface TCR$\gamma\delta$ and CD3 expression (Fig 2 b,d). To interrogate which markers were significantly differentially expressed, thus contributing to the cluster segregations, we applied conventional flow cytometry to independent cohorts of mice, since detection reagents for individual markers are not constrained by overall panel composition.

CD103, a signature component of TGFβ-regulated T_{RM} cells, was significantly upregulated by epidermal and dermal $\gamma\delta^X$ cells (Fig 2e-g; see also Fig 1e), and from spectral analyses it was evident that most epidermal $\gamma\delta^X$ cells were CD103^{hi} (Fig 2b), while essentially all dermal $\gamma\delta^X$

cells expressed at least as much CD103 as did TCR$\gamma\delta^+$ cells and frequently more (Fig 2d). By contrast, CD69, a tissue-resident T cell hallmark, was significantly downregulated (Fig 2e-g) with spectral data again depicting this as true for essentially all $\gamma\delta^X$ cells; note, almost complete correspondence of reduced CD69 expression with reduced CD3 or TCRδ expression (Fig 2b), and with induced gfp expression for dermal cells (Fig 2d). This is not to ignore some phenotypic overlap, for example, there were TCR$\gamma\delta^+$ cells in control mice that were CD103^{hi} and/or CD69^{lo} (Fig 2e). Epidermal and dermal $\gamma\delta^X$ cells also significantly downregulated Tigit and Lag3, with epidermal $\gamma\delta^X$ cells additionally acutely downregulating ICOS (Fig 2e) and Tim3 (Supp Fig 2a) and showing the loss of a 4-1BB^{hi} (CD137^{hi}) subset (Supp Fig 2b), as observed in Skint1-blockaded mice[25].

In sum, sustained TCR expression was essential for regulating cell surface expression levels of several profoundly important immune regulators, a subset of which was comparably TCR-dependent in epidermal and dermal $\gamma\delta$ T cells despite those cells being very different from each other. Thus, we next used transcriptomics to investigate more broadly the real-time TCR-dependencies of $\gamma\delta$ T cell phenotypes.

The nature and impact of TCR$\gamma\delta$-regulated genes

Whereas our previous application of single cell RNA-Seq resolved the heterogeneity of steady-state DETC transcriptomes into 4 clusters[25], it was much less effective at distinguishing DETC from unmanipulated versus Skint1-blockaded mice, largely because there were few differentially expressed genes (DEGs). Thus, to first assess the scale of differential gene expression across $\gamma\delta^X$ and $\gamma\delta^{TCR}$ epidermal lymphocytes, a pilot comparison was undertaken using the NanoString N-Counter 770-gene cancer immune profiling panel. Conspicuously, only two genes were significantly altered: *Lag3* was decreased in $\gamma\delta^X$ cells, completely consistent with flow cytometry (above), and mRNA encoding integrin alpha 6 (*itga6*) was upregulated (Supp Fig 3a). Based on this, we anticipated few transcriptional differences between $\gamma\delta^X$ and $\gamma\delta^{TCR}$ cells, in which setting bulk RNA-Seq is the preferred method.

By principal component analysis (PCA), PC1 which contained most of the variance showed complete segregation of $\gamma\delta^{TCR}$ and $\gamma\delta^X$ transcriptomes in both epidermis and dermis (Supp Fig 3b). Note that for epidermis, only age-matched males were examined, and that for dermis, which included a mixture of male and female mice, the differences in PC1 were not attributable to sex. Validating these comparisons were profound reductions of *Trgc1* and *Trgv5* transcript

counts in epidermal γδ^{X} cells, and of *Trgc1*, *Trgv4,* and *Trgv6* transcripts in dermal γδ^{X} cells, while γδ^{X} cells from both sites showed significantly upregulated *Trgc3* expression, as considered above (Supp Fig 3c).

To confirm that upregulated *Trgc3* transcripts did not encode new TCR protein, we assessed TCR proteins *via* a low-input, high-resolution proteomic analysis of epidermal CD45^{hi}Dump^{neg} lymphocytes sorted from γδ^{TCR} and γδ^{X} mice one week after tamoxifen administration. In addition to the greatly reduced expression of TCR-Cγ1 (Supp Table 1), there was significantly reduced expression of TCR-Vδ4 (a.k.a. Vδ1) and TCR-Cδ, that jointly pair with Vγ5-Cγ1, and of CD3γ (Supp Table 1), presumably reflecting the reduced stability of proteins chains directly contributing to TCR complexes. Importantly, no signals were attributable to TCR-Cγ3, consistent with *Trgc3* being a pseudogene: thus, messages spliced to it from VJγ would not impact cell phenotypes.

Beyond TCR gene expression there were only ~300 statistically significant DEGs when comparing epidermal γδ^{X} and γδ^{TCR} cells: 145 downregulated and 156 upregulated, with 11723 genes unaffected (Fig 3a, b; note *Trgc1* was so downregulated in epidermis and dermis to be off the "padj" scales of Fig 3a). By contrast, dermal γδ^{X} cells displayed 4454 DEGs; 1947 downregulated and 2507 upregulated, with 10751 genes unaffected (Fig 3a, b). Thus, in both γδ T cell types, steady-state γδTCR expression is an essential regulator of gene expression, but to very different degrees, with the lesser impact being on cells that previously underwent Btnl-dependent, TCR-mediated repertoire selection.

By gene set enrichment analysis (GSEA), epidermal γδ^{X} cells showed significant albeit weak upregulation of genes classified as "TNF signalling via NFκB" (Fig 3c; Supp Fig 3d), to which prominent contributors are some mRNAs ordinarily expressed by activated-yet-resting mouse tissue-intrinsic γδ cells, e.g., *Btg2*, *Junb, Fos*. By contrast, there was significant and substantial downregulation of gene sets: "Myc targets", "E2F targets", "G2M checkpoint" and "mitotic spindle". Of note, the last three of these gene sets were also downregulated by DETC (which concurrently became rounded) in mice one day post-exposure to uvb irradiation[25]. These changes strongly suggest that a small subset of genes regulating the cells' activation status are under acute TCR control.

Interestingly, "Myc targets" and "mitotic spindle" genes were likewise among the most dysregulated genes in dermal $\gamma\delta^X$ versus $\gamma\delta^{TCR}$ cells, albeit that the latter genes were overall upregulated following TCR ablation (Fig 3c; Supp Fig 3d). Despite this collective difference, there was some consistency at an individual gene level, with the few mitotic spindle genes significantly upregulated in TCR-ablated DETC being likewise upregulated in dermal $\gamma\delta^X$ cells (Supp Table 2). Of note *Rasa2*, which when ablated improves CAR-T cell activation[33], was downregulated in both cell types, evidencing its acute regulation by the TCR. Additionally, there was substantial downregulation in dermal $\gamma\delta^X$ cells of "fatty acid metabolism" and "oxidative phosphorylation" (Fig 3c; Supp Fig 3d), which seems noteworthy given that oxidative phosphorylation is the major metabolic pathway of systemic Vγ4$^+$ cells that produce IL-17[34], as do dermal $\gamma\delta$ T cells. Moreover, TCR$\alpha\beta^+$ T_{RM} cells require fatty acids for their metabolism[35], although this has not hitherto been attributed to TCR signalling.

Conspicuously, several DEGs correlated with the changes in cell-surface phenotypes of $\gamma\delta^X$ cells: thus, *Tigit* and *Cd69* mRNAs were significantly downregulated in epidermal and dermal $\gamma\delta^X$ cells, and *Tnfrsf9* encoding 4-1BB (CD137) was downregulated in epidermal $\gamma\delta^X$ cells (Fig 3d). Likewise, *Itgae* that contributes to encoding CD103 was upregulated in dermal $\gamma\delta^X$ cells (Fig 3d). Nonetheless, correlations were not universal, re-emphasising that for many genes, RNA and protein expression do not align[36]. Thus, *Itgae* was not consistently upregulated in epidermal $\gamma\delta^X$ cells, almost all of which upregulated CD103 protein (above), while *Cd28* mRNA was downregulated in epidermal and dermal $\gamma\delta^X$ cells despite the fact that surface CD28 was undetectable on either. Likewise, significant changes in surface expression of Tim3, Lag3 and ICOS, reported above, were not consistently reflected in transcriptional changes. Hence, acute TCR-dependent regulation operates at transcriptional and post-transcriptional levels.

Beyond the cell surface, there was consistent upregulation of *Jun* and *Junb* encoding early-response transcription factors regulating the cells' activation state, and implicated in TCR signalling in gut $\gamma\delta$ IEL[37]. There was also consistent downregulation of transcripts encoding the effector chemokine, Xcl1 (Fig 3d), that mediates skin $\gamma\delta$ T cell recruitment of conventional type 1 dendritic cell (cDC1) in the response to mCMV[38], that is crucial for cDC1 recruitment to murine tumours[39], and that is also highly expressed by so-called T_{PEX} cells that fuel CD8$^+$ T cell proliferation following immune checkpoint blockade therapy[40,41]. Among chemokine mRNAs, *Ccl5* was also significantly upregulated in TCR-ablated DETC (Fig 3d), whereas regarding cytokines, dermal and epidermal $\gamma\delta^X$ cells shared significant upregulation of steady-state *Il13*

transcripts (Fig 3d), which are also upregulated during nutrient deprivation[42]. Hence, despite there being an order of magnitude difference in the number of DEGs in epidermal and dermal $\gamma\delta^X$ cells, respectively, *Jun*, *JunB*, and *Il13* upregulation and *Tigit, Cd69* and *Xcl1* downregulation composed a conserved core of TCR-regulated changes in both cell types.

Additionally, dermal and epidermal cells shared slight but significant downregulation of *Klrb1a* and *Klra5* (encoding Ly55a and Ly49, respectively), while epidermal DEGs additionally included *Klrc1* (encoding NKG2A) downregulation and *Klra7* (encoding Ly49g) upregulation (Fig 3d). These gene-products are examples of NKRs and Killer inhibitory receptors (KIRs) that collectively contribute to the innate regulation of cytolytic lymphocyte activity (considered further below).

Given the real-time TCR-dependence of several genes in epidermal and dermal $\gamma\delta$ T cells, we then asked whether there might be overt physiological consequences of acute TCR deletion. Indeed, within two weeks of tamoxifen administration, $\gamma\delta^X$ mice showed significantly increased trans-epidermal water loss (TEWL), an established parameter of epidermal integrity: *de facto*, the readings taken from $\gamma\delta^X$ and $\gamma\delta^{TCR}$ mice barely overlapped (Fig 3e). This rapid physiological impact of acute TCR deletion in local T cells was not attributable to an induced pro-inflammatory state because there was at that time-point no significant difference in ear thickness (Fig 3f).

Contrasting TCR$\gamma\delta$-dependence in gut and skin

Having established a core TCR-dependency of divergent $\gamma\delta$ T cells in the skin, we next investigated the consequences of acute TCR deletion in the gut. Confocal micrographs of $\gamma\delta^X$ mTmG and $\gamma\delta^{TCR}$ mTmG mice at 4 weeks after tamoxifen treatment revealed fewer gfp^+ cells in $\gamma\delta^X$ mTmG mice, with the average number decreasing from ~30 to <15 per villus (Fig 4a, b). This cell loss, not seen in skin, probably reflects the fact that gut $\gamma\delta^+$ IEL but not skin $\gamma\delta$ cells can be reconstituted from postnatal progenitors. Thus, in $\gamma\delta^X$ mice, natural IEL turnover would be evident, with the cells replaced over time with $gfp^{neg}V\gamma7C\gamma1^+$ cells developing from progenitors in which $TCR\delta^{creERT}$ would not have been active. However, such cells would not be distinguishable *prima facie* from mature $gfp^{neg}V\gamma7C\gamma1^+$ IEL in which Cre had been poorly penetrant. We therefore used $Rosa26^{CreERT}$ which is ~100% penetrant, thereby preventing the generation and influx of replacement $V\gamma7C\gamma1^+$ cells. Whereas $dump^{neg}CD103^+$ cells of $\gamma\delta^{TCR}$ mice were mostly $V\gamma7^+$ cells, as anticipated, this was reduced by ~90% in $\gamma\delta^X$ mice (Supp Fig 4a), and while there

was no replacement by αβ IEL, since their representation remained comparable in the two strains (Supp Fig 4b), there was a significant inversion in the frequencies of Cγ1$^+$ *versus* Vγ1Cγ4$^+$ cells, the latter being the only major γδ cell subset whose progenitors will not have lost the capacity to express TCRγδ (Supp Fig 4c). Hence, the TCR is required in real-time for the maintenance and turnover of the prototypic gut γδ IEL compartment.

In addition, we assessed γδ^X gfp$^+$ cells for Fas expression, since *Fas*-deficient mice cannot stably retain Vγ*7*$^+$ IEL in the gut[43]. Indeed, flow cytometry showed striking Fas (CD95) downregulation in γδ^X mice versus γδ^{TCR} mice (Fig 4c), added to which a preliminary NanoString analysis of gut lymphocytes (prepared by a protocol that enriches for IEL) showed downregulated *Fas* transcripts in γδ^X mice versus γδ^{TCR} mice, while there was upregulated *Sell* that encodes L-selectin, a systemic lymphoid homing molecule (Supp Fig 4d). In short, *Fas* may be a TCR-dependent gut retention factor. Addtionally, *Klra7* was also upregulated, as it was in the epidermis (above).

Affirming the difference of intestinal lymphocytes in γδ^X and γδ^{TCR} mice, spectral flow showed striking segregation according to genotype, which was validated *a posteriori* by CD3, TCRγδ, Vγ*7*, and Vγ4 expression (Fig 4d). Note, the excess of Vγ*7* over Vγ4 in γδ^{TCR} cells confirmed that our methods primarily enriched for IEL. As in skin, CD103 expression was either retained or upregulated in γδ^X IEL while CD69 was collectively downregulated (Fig 4d, e). There was also downregulation of CD27, CD44, Tigit, and also CD122 (IL2Rβ) which was likewise downregulated in Vγ*7* IEL of mice acutely depleted of *Btnl1*[20]. Again, there were phenotypic overlaps, e.g., clusters of CD44^{hi} γδ^X cells, as evidenced from spectral flow (Fig 4d).

To interrogate the basis for these phenotypic changes, we again used bulk RNA-Seq, comparing CD45^{hi}dump^{neg} cells from γδ^X and γδ^{TCR} mice. Once more, PC1 that carried the bulk of the variance showed that transcriptomes segregated according to genotype (Supp Fig 4e), independently of segregation by sex, and there was, as expected, profound downregulation of *Trgc1, Trgv7* and *Trgv4,* and upregulation of *Trgc3* (Supp Fig 4f) Strikingly aligned to their *Btnl*-(*Skint*)-selected epidermal counterparts, γδ^X IEL displayed relatively few statistically significant DEGs: *77* upregulated; 63 downregulated, versus 12,683 unchanged (Fig 4f). Furthermore, downregulated genes included *Tigit* and *Xcl1* while *Jun* and *Junb* were upregulated (Fig 4g), completely aligned with epidermal and dermal data. Also in common was downregulation of several genes encoding KIRs, including *Klre1* (encodes NKG21), *Klra6* (Ly49F), *Klra3* (Ly49C), and *Klrh1* (Fig 4g).

By GSEA, the subsets of genes most significantly downregulated by acute TCR deletion included "Myc targets" which were among those most significantly downregulated in epidermal and dermal $\gamma\delta^X$ cells (Supp Fig 4g). Likewise, "oxidative phosphorylation" was downregulated in gut IEL (Supp Fig 4g), as it was in dermal $\gamma\delta^X$ cells (above). Gene-sets are defined by many genes, but in this regard, it was striking that when we selected mRNAs significantly downregulated in at least three of four gut $\gamma\delta^X$ samples, there was considerable correspondence with those down-regulated in all three dermal samples (Supp Table 2). Thus, notwithstanding the fact that multiple criteria diistinguish $\gamma\delta$ T cells in the epidermis, dermis, and gut, they shared several acutely TCR-dependent genes and proteins.

Real-time TCR-dependent regulation of chromatin accessibility

The status of a cell at steady-state and its poise to respond to challenge will be regulated epigenetically. We therefore applied ATAC-Seq to epidermal and intestinal IEL to ask whether aspects of chromatin accessibility show real-time TCR dependency (note: dermal cells could not be recovered in sufficient numbers for this analysis). Whereas most peaks of shared chromatin accessibility were of comparable frequency (peak heights) in $\gamma\delta^{TCR}$ and $\gamma\delta^X$ cells (31,373 in epidermis; 26,136 in gut), a small percentage was represented significantly differently according to genotype in both tissues (Fig 5a, b).

Correlations with DEGs were inexact given that epidermal and gut $\gamma\delta^X$ cells had comparable numbers of TCR-dependent DEGs, but contrasting numbers of loci with significantly altered chromatin accessibility (Fig 5a, b). Nonetheless, those loci included core DEGs identified above. Thus, the *Jun* and *JunB* loci showed greater accessibility in $\gamma\delta^X$ mice, consistent with increased expression (Supp Fig 5a-d). The same was true of *Ccl5* and *Il13* in $\gamma\delta^X$ epidermal lymphocytes (Fig 5c, d). Nonethless, a strikingly atypical pattern was evident for *Tigit* and *Xcl1* (Fig 5e-h), with reduced expression associated with increased chromatin opening. This would be consistent with factor(s) downstream of steady-state TCR signalling occluding repressors that can then bind DNA more readily at these loci in $\gamma\delta^X$ cells (see Discussion). In sum, acute TCR ablation in skin and gut IEL rapidly translated to altered chromatin configurations, albeit at a small percentage of loci.

TCR-dependent regulation of Human V$\delta1^+$ cells

Having identified a core set of genes and proteins regulated by sustained TCR expression across divergent γδ T cells in mouse skin and gut, we asked whether this pattern might be evolutionarily conserved. To this end, we examined γδ T cells in which we could delete Vδ1, the main γδ TCR chain associated with human tissue-intrinsic γδ cells, akin to the association of Cγ1 with mouse tissues. Confounding this goal is a requirement for reiterative TCR stimulation in existing protocols for expanding human Vδ1 cells[44]. Therefore, to seek a TCR-independent means of establishing Vδ1 cells, we turned to HTLV1-immortalised Vδ1$^+$ cell lines[45]. HTLV1-immortalisation will inevitably alter the phenotype of Vδ1$^+$ cells relative to counterparts *in vivo* and might be expected to nullify any steady-state requirement for the TCR. Nonetheless, we used CRISPR and specific external guide sequences to acutely delete the TCR by generating an INDEL in *TRDV1* that encodes TCR Vδ1 (Supp Fig 6a).

After several optimisations, a protocol was developed that, albeit with incomplete penetrance, generated Vδ1^{neg} cells (Supp Fig 6b-d). To insulate our studies from potential growth disadvantages of TCR-ablated cells, we applied flow cytometry to two sets of cultures only 10 days post-CRISPR, to achieve 94%-97% enrichment of Vδ1^{neg} cells (Supp Fig 6e; note, that Vδ1^{neg} cells were also CD3^{neg}, in contrast to *Trgc1*-deficient DETC; Supp Fig 1e), and immediately compared their transcriptomes to those of residual TCR-Vδ1$^+$ cells (Supp Fig 6b).

By PC1 (that accounted for >90% of the variance) the transcriptomes again segregated according to genotype (Fig 6a). As depicted in the volcano plot, there were ~1400 DEGs; almost evenly split into those upregulated and downregulated, respectively, in TCR^{neg} cells (Fig 6b). Of note, the number of DEGs more closely resembles the DEGs of dermal γδ T cells, that lack a known TCR-selecting element. Strikingly, the DEGs included several genes of immunological significance including *TIGIT* and *XCL1* (Fig 6b, c) that were downregulated, exactly as observed in each of the mouse γδ^x populations examined. Also conserved was downregulation of several KIR/NKR genes, that in human TCR^{neg} cells included *KLRD1* (CD94), *KLRB1* (CD161), and *KLRK1* (NKG2D), together with *GZMA, GZMK* and *CR-TAM* (Fig 6b, c), all of which collectively contribute to the regulation of cytolytic responses particularly associated with innate lymphocytes. Additionally, *IL13* was upregulated (Fig 6b, c), as it was in epidermal and dermal γδ^X cells, while *TNFRSF9* (4-1BB) was downregulated, as it was in epidermal γδ^X cells. *SCART1* was also upregulated (Fig 6b, c), as were several genes that, like *Il13*, are associated with Th2 T cell biology, including *IL5*, *IL9*, *IL17RB* (see Discussion).

By GSEA, the pathways most overtly dysregulated in TCR^{neg} versus TCR^{+} cells were "fatty acid metabolism" and "oxidate phosphorylation" (Fig 6d), within which pathway, many of the DEGs were also significantly dysregulated in dermal and gut $\gamma\delta^{x}$ cells, some equivalently (Supp Table 2). Because they are stably immortalised, the human $V\delta1^{+}$ cells offered the opportunity to seek functional parallels of gene expression changes. To this end, the metabolism of two independent TCR^{neg} lines (C4, C5) was compared to parental $V\delta1^{+}$ cells (D2) using extracellular flux analysis. Despite being immortalised by HTLV1, both TCR^{neg} lines showed reduced metabolic activity compared to parental D2 cells, as reflected in lower basal oxygen consumption rates (OCR) and extracellular acidification rates (ECAR) (Fig 6e[i], f[i]). Although they displayed reduced ATP-coupled respiration at baseline, the TCR^{neg} lines had comparable spare respiratory capacity (Fig 6e[ii], f[ii]). However, by contrast to the parental line, this reserve was greatly diminished in the TCR^{neg} lines when fatty acid oxydation (FAO) was inhibited by etomoxir (Fig 6e[iii]; f[iii]), with EACR also more sensitive to etomoxir treatment in TCR deficient cells. Hence, TCR loss appeared to increase FAO dependence, consistent with upregulation of the corresponding gene-set.

In sum, even in virus-immortalised human $V\delta1^{+}$ T cells, sustained TCR$\gamma\delta$ expression regulated the steady-state expression of several genes and proteins that included components of a core subset identified in mice. Indeed, the sole exceptions were *JUN* and *JUNB*, the regulation of which can be expected to be overridden by virus immortalisation. Moreover, virus immortalisation did not overide steady-state impacts of TCR$\gamma\delta$ on cellular metabolism that were likewise implied for murine intestinal IEL and dermal $\gamma\delta$ T cells by their altered transcriptomes.

Signature innate responses of TCR-deleted cells *in vitro*

The next question was whether TCR$\gamma\delta$ was required in real-time for immunosurveillance responses to challenge. By stimulating dermal cell preparations with PMA plus ionomycin that potently activates signalling pathways downstream of the TCR, it was clear that comparable percentages of $\gamma\delta^{X}$ and $\gamma\delta^{TCR}$ cells had the potential to produce IL-17, although the amount of IL-17 per cell seemed slightly less for $\gamma\delta^{X}$ cells, as judged by gMFI (Supp Fig 7a).

We next examined a signature innate response of skin $\gamma\delta$ T cells to cytokines alone. Thus, we prepared skin TCR$\gamma\delta^{+}$ cells (dermis plus epidermis) from $\gamma\delta^{TCR}$ mice, and counterpart TCR$\gamma\delta^{neg}$gpf^{+} cells from $\gamma\delta^{X}$ mice and compared the cells' responsiveness to IL-12 + IL-18, which has the potential to induce IFNγ, and to IL-1β + IL-23, which induces IL-17. By staining

permeabilised cells treated with brefeldin A (so as to retain intracellular cytokines), we detected comparable IL-17 production by $\gamma\delta^{TCR}$ and $\gamma\delta^{X}$ cells, typical of dermal Vγ4 and Vγ6 cells. Conversely, there were few $\gamma\delta^{TCR}$ IFNγ-producers, reflecting the fact that whereas DETC are skewed against IL-17 production they are recalcitrant IFNγ producers (Fig 7a), although, despite this, some IFNγ production was evident for $\gamma\delta^{X}$ cells (Fig 7a). Improved IFNγ production by DETC has been previously observed following the cells' adaptation to short-term culture, and in this setting too there was a stronger response of epidermal $\gamma\delta^{X}$ cells from which the TCR had been deleted by tamoxifen exposure *in vitro* (Supp Fig 7b).

When gut IEL were harvested and incubated with IL-12 + IL-18 they readily produced IFNγ, which was reduced by about 50% for $\gamma\delta^{X}$ IEL (Supp Fig 7c). IL-1β + IL-23 failed to induce IL-17 production (Supp Fig 7c), consistent with IEL skewing. We could conclude that acute TCR deletion did not alter the signature functional skewing of the tissue-intrinsic γδ subsets examined, and had little consistent impact on the innate capacity to produce effectors in response to defined cytokines alone.

Real-time TCRγδ-dependent immunosurveillance

In vivo, the prototypic example of innate immunosurveillance of tissue perturbation by dermal IL-17-producing γδ T cells is the response to epicutaneous application of Aldara cream. Containing a ligand for Toll-like receptor (TLR) 7, Aldara (a.k.a. Imiquimod) stimulates myeloid cells to release IL-1β and IL-23 that jointly induce release of IL-17 by co-located dermal γδ T cells. In turn, the IL-17 elicits neutrophil recruitment, leading to significant, psoriaform skin-thickening over a 4-5 day period, as evidenced for treated $\gamma\delta^{TCR}$ mice (Fig 7b; Supp Fig 7d). By comparison, neutrophil recruitment and skin thickening were almost entirely ablated in $\gamma\delta^{X}$ mice exposed to Aldara just 7 days after tamoxifen treatment was ceased (Fig 7b; Supp Fig 7d). Moreover, Aldara treatment of Nur77.gfp mice significantly increased skin γδ T cell expression of gfp, a reporter of TCR signalling[46] (Supp Fig 7e). These datasets collectively demonstrate that despite the capacity of dermal $\gamma\delta^{X}$ cells to produce IL-17 *in vitro*, the cells were unable to promote the prototypic innate γδ T cell response to Aldara *in vivo*. Rather, Aldara treatment upregulated signalling from TCRγδ which proved essential to elicit signature psoriaform pathology.

Another prototypic challenge is ultraviolet irradiation which rapidly increases the frequency of DETC that express high levels of the activation markers, 4-1BB, CD122, and ICOS. These *in vivo* responses were also blunted in $\gamma\delta^{X}$ mice irradiated 7 days after 7 days of tamoxifen treatment, with the ICOS response being essentially ablated, together with the capacity to induce a 4-1BB^{hi} subset associated with activation[25] (Supp Fig 7f). Thus, TCR$\gamma\delta$ was also required for the signature DETC response to epicutaneous u.v. irradiation.

Finally, we examined skin immunosurveillance responses to cancer. Subcutaneous infusion of B16.F10 melanoma cells into C57.BL/6 mice is followed within one to two weeks by tumour formation which is not readily controlled by endogenous T cells, even when immune checkpoints are applied[47]. Nonetheless, a natural, beneficial role for $\gamma\delta$ T cells is inferred from $\gamma\delta$ T cell-deficient mice developing larger tumours more rapidly than control mice[48]. To examine whether this response was affected by acute TCR deletion, we undertook two sets of experiments, injecting tumour cells within 5 days of tamoxifen treatment of $\gamma\delta^{TCR}$ mTmG and $\gamma\delta^{X}$ mTmG mice, respectively (n=71). We observed tumour formation in 80% of $\gamma\delta^{TCR}$ mice (28 / 35), whereas tumour incidence in $\gamma\delta^{X}$ mice was >97% (35 / 36) with the modal tumour size also being significantly greater (Fig 7c). This significantly impaired capacity to control melanoma did not reflect a lack of intratumoral gfp^{+} $\gamma\delta^{TCR}$ or $\gamma\delta^{X}$ cells, since those were rare in both cases, and nor did it reflect a failure to promote tumour surveillance by intratumoral CD45^{+} $\alpha\beta$ T cells since their frequencies were comparable in both strains (Supp Fig 7g). Indeed, draining lymph node cellularity was higher in $\gamma\delta^{X}$ mice (Supp Fig 7h), presumably reflecting persistent stimulation by larger tumours. We conclude that there is a natural capacity of $\gamma\delta$ T cells to survey and limit melanoma growth, and this depends in real-time on TCR$\gamma\delta$.

To examine whether $\gamma\delta^{X}$ cells were defective in interacting with B16.F10 cells, we undertook two experiments. Thus, we cultured B16.F10 cells, first with DETC freshly isolated from tamoxifen-treated $\gamma\delta^{TCR}$ mice and $\gamma\delta^{X}$ mice, and second with short-term DETC cultures from $\gamma\delta^{TCR}$ mice and $\gamma\delta^{X}$ mice that were treated with tamoxifen *in vitro* to delete the TCR (see above). In both cases, the induction of apoptosis in B16.F10 targets (measured by either Annexin V or caspase 3 staining) was not ablated but was significantly impaired by acute TCR loss (Fig 7d-f). Of note, this real-time TCR-dependence of target cell cytolysis seemed to be evolutionarily conserved, in that relative to TCR$\gamma\delta^{+}$ HTLV1-immortalised V$\delta1^{+}$ cells, TCR$\gamma\delta^{neg}$ cells showed significantly impaired capacity to target a colorectal carcinoma cell line, HT29 (Fig 7g).

Discussion

Ablating the TCR for at most a few days had wide-ranging pathophysiological consequences, including impaired capacity to regulate cutaneous water balance; deficient responses to DNA damage or to cancer cells, thereby permitting excessive tumour growth; and a failure to rapidly induce psoriaform pathology. These data unequivocally demonstrate an active tissue surveillance system that depends on TCRγδ in real-time, in addition to any prior, TCR-dependent developmental preprograming that may condition γδ T cells to respond innately[15].

Our findings resolve a long-standing "γδ paradox": whereas rapid, nonclonal γδ responses had been attributed to TCR-independent innate activation by cytokines and/or NKRs[13], phenocopying NK cells and ILC, the responses evidently retain a real-time TCR dependence. In response to Aldara *in vivo*, TCRγδ clearly provided γδ cells a capacity to produce IL-17. Given our data on metabolism, TCRγδ may provide competence for a necessary switch to glycolysis for IL-17-producing γδ T cells in psoriatic conditions[49]. Alternatively, but not mutually exclusively, TCRγδ possibly overcomes checkpoints which are absent *in vitro* but which may be exerted by the tissue microenvironment *in vivo*: identifying such checkpoints should be a priority.

A modality of overcoming repression may align with a possible potential of the TCR to block transcriptional repression of *Xcl1* and *Tigit* which we infer from the data presented here, and which might likewise apply to other genes. Repressor removal can be the fastest means to upregulate genes, potentially consistent with which, γδ TCR stimulation very rapidly upregulates Tigit and Xcl1. Such activities of TCRγδ are clearly distinct from tonic signalling described for αβ TCRs, that requires some components of clonotypic ligands, e.g., MHC, and that regulates cell survival, which was not universally the case here[50].

Inevitably, TCR-dependence should be considered in the context of ligands. Indeed, Aldara stimulation was reported to expand IL-17-producing Cγ1$^+$ γδ T cells, which then responded better to secondary stimulation, a hallmark of adaptive immunity[51,52], although neither study assessed either TCR-dependence or ligands. Likewise, other immunosurveillance settings may depend on TCR activation by stress-ligands, e.g., EPCR[11].

In other cases, the requirement may be for TCRVγ-specific BTNL ligands. Notably, acute Skint1 blockade or Btnl1 ablation[20,25] closely phenocopied the impacts of acute TCR ablation on

epidermal and intestinal T cells, respectively. Nonetheless, they were not obviously identical. Thus, acute Btnl1 ablation did not induce gut-specific depletion of γδ T cells observed following Cγ1 ablation, which possibly highlights an under-considered, TCR-dependent role of Fas-FasL[43], likely applicable to human gut Vγ4$^+$ cells that share many parallels with mouse Vγ7$^+$ IEL[21,23]. Similarly, increased TEWL in Skint1-blockaded mice could not be disentangled from skin inflammation[25], whereas it could in γδ^x mice, presumably because TCR-Cγ1 ablation also inactivates pro- inflammatory dermal γδ cells[53]. Additionally, acute Btnl1 or Skint disruption did not obviously affect KLR expression profiles. Possibly, these additional impacts of TCR-Cγ1 ablation reflect loss of responses to clonotypic ligands that BTNL-reactive human and mouse γδTCRs have been shown to have[54].

However, no known Btnl-equivalents exist for dermal Vγ6Vδ1 TCRs, that may instead be polyreactive[55]. Nonetheless, such reactivities were not placed into the context of real-time TCR-dependence in non-challenged mice, as observed here. Moreover, human Vδ1 cells showed TCR-dependence even in culture, which possibly reflects ligand-independent γδTCR signalling for which precedent exists[56]. Either way, it now seems highly unlikely that there are any tissue-intrinsic γδ T cell compartments that do not depend on ongoing TCR signalling, and hence for γδ T cell-mediated immunosurveillance to occur, a cancer or other lesion must be conducive to TCR function, whether or not this includes ligand provision. This must inform the therapeutic deployment of γδ T cells.

For Vγ5$^+$ DETC and Vγ7$^+$ gut IEL, that undergo developmental TCRVγ chain-dependent selection, barely a few hundred genes tiny showed real-time TCR-dependence, as if the TCR already played a major part *en route* to the cells' steady-state maturation. To put this into context, 6337 DEGs distinguished systemic mouse IFNγ-producing from IL-17-producing cells[57]. Although not at this scale, dermal γδ cells showed much greater real-time impact of TCR ablation than BTNL-selected cells, akin to conventional resting T cells, despite their commonly displaying preactivation-associated markers, e.g., CD44[58]. Blood-derived human Vδ1 cells, for which there is also no known TCR-mediated selection element, also showed many TCR-dependent DEGs, although conclusions need to be qualified by the cells' virus-immortalised status[59]. Interestingly, there was also unexpected cell type-specific variation in the impact of TCR-ablation on CD3 protein expression.

Given the differences in their degrees of TCR-dependence, it was striking that diverse γδ cell types, including an immortalised human Vδ1 cell line, shared a core phenotype connecting the TCR to blue-ribband immune regulators, specifically: TIGIT and KLRs that regulate cell responsiveness; Xcl1 which contributes to priming immune responses in tissues and to proliferative T cell bursts[41]; IL-13 implicated in maintaining tissue integrity; CD103 and CD69 that contribute to homing and tissue-localisation; and Jun and JunB that regulate cell state, often under stress, and with potential to increase FAO via CPT1A gene regulation[60]. Although the direction of TCR-dependent regulation varied according in different γδ cell types, these specific pathways were repeatedly affected by TCR ablation, by contrast to others, e.g., functional skewing, for which there was no apparent real-time requirement for continued TCR expression.

TCR ablation did not simply revert T cells to wholly innate or immature states, e.g., by upregulating PLZF, Rorγc, and Bhlhe40, or *Rag1 / Rag 2*, and it did not necessarily induce novel states: for example, γδ^{x} DETC showed several transcriptional and morphological changes akin to w.t. DETC from u.v.-irradiated mice that may reflect pathophysiologic transitions in TCR-mediated regulation[25]. Strikingly, TCR-dependent effects had impacts on chromatin, transcription, and surface protein expression, that commonly seemed independent of each other.

Consistent upregulation of CD103, which is TGFβ-regulated, may reflect the fact that TCR signals ordinarily moderate the impact of tissue-processed TGFβ which is required for T_{RM} cells but which in excess could be immunosuppressive[61]. This will be germane to surveillance of TGFβ-rich microenvironments, a major issue in cancer immunotherapy. Universal *Il13* upregulation evokes its upregulation *in vivo* during nutrient deprivation[42], together with several other Th2-associated cytokines that were also upregulated in the TCR-ablated human Vδ1 cells that we generated. These factors may contribute to wound-healing, and we concur with speculation that under metabolic stress, cytolytic and Th1-immune functions may become secondary to functions sustaining tissue integrity.

In sum, our findings show an unequivocal real-time dependence of tissue-intrinsic γδ T cells on TCRγδ function, questioning the classification of prominent γδ T cell subsets as innate. However, the TCR-dependence also may not be typically adaptive, i.e., driving clonal expansion and memory. Rather, it may in part sustain polyclonal competences, e.g., metabolic adaptability, or responsiveness to Type I IFN[37] or other stimuli. Thus, our findings seemingly extend the prism through which TCR biology should be viewed, with inevitable potential to improve γδ T cell-

based immunotherapies including those utilising Vδ1$^+$ cells, by ensuring that target lesions are strongly conducive to TCR signalling[3].

Acknowledgements

We thank P. Vantourout, L. Monin, B. Silva-Santos, S. Mensurado, N, Gonçalves Sousa, JR Regueiro for helpful advice and discussions and E. Theodoridis, C. Watkins, P. Owers and C. Brown for logistical support. We are grateful to M. Buck (Crick) for guidance in extracellular flux analysis; to D. Schneider-Luftman, P. Soro Barrio, and P. Chakravarty for data analysis assistance; to A. Agua-Doce, S. Namjou, and P. Hobson for expertise in cell sorting and analysis; and to T. Auchynnikava for contributions to proteomic analyses. We thank the Flow Cytometry and Fluorescence Microscopy Unit, CAI of Biological Techniques, Complutense University of Madrid, for assistance and technical support. A.H. received support from the Francis Crick Institute, which receives core funding from Cancer Research UK (grant no. FC001093), the Medical Research Council (MRC) (grant no. FC001093) and the Wellcome Trust (grant no. FC001093). N.V is supported by a sponsored research agreement with Takeda. M.M-R was supported by funding from the Agencia Española de Investigación (AEI) (PID2022-139095OA-I00 and RYC2021-034348-I) and Fundación Fero (IV Ayuda de Investigación en Cáncer FERO-ASEICA). A.Z-C. was supported by an AEI predoctoral fellowship (PREP2022-000845). B.G-C is supported by Ministerio de Ciencia, Innovación y Universidades (BG23-00019). A.V.M., was supported by funding from AEI (PID2021-125501OB-I00).

Author contributions

A.H. and M.M-R. conceptualized the study. N.V., B.G-C., and M.M-R. devised the methodology and managed the resources. N.V., B.G-C., A.Z-C., AM.M., D.R.M., A.J., J.F., A.V.M., R.A., and M.M-R. carried out the investigation. N.V., B.G-C., A.Z-C., AM.M., D.R.Mc., A.J., R.A., A.H. and M.M-R. carried out the data analyses. A.H., N.V., and M.M-R wrote the original manuscript draft. All authors reviewed and edited the manuscript draft. A.H. and M.M-R acquired funding.

Competing interests

N.V. is currently employed on a sponsored research agreement with Takeda Pharmaceuticals. A.H. receives laboratory research funding from Takeda Pharmaceuticals (starting in February 2023). The remaining authors declare no competing interests.

Bibliography

1 Gentles, A. J. *et al.* The prognostic landscape of genes and infiltrating immune cells across human cancers. *Nat Med* **21**, 938-945, doi:10.1038/nm.3909 (2015).

2 Silva-Santos, B., Mensurado, S. & Coffelt, S. B. gammadelta T cells: pleiotropic immune effectors with therapeutic potential in cancer. *Nat Rev Cancer* **19**, 392-404, doi:10.1038/s41568-019-0153-5 (2019).

3 Hayday, A., Dechanet-Merville, J., Rossjohn, J. & Silva-Santos, B. Cancer immunotherapy by gammadelta T cells. *Science* **386**, eabq7248, doi:10.1126/science.abq7248 (2024).

4 Wu, Y. *et al.* An innate-like Vdelta1(+) gammadelta T cell compartment in the human breast is associated with remission in triple-negative breast cancer. *Sci Transl Med* **11**, doi:10.1126/scitranslmed.aax9364 (2019).

5 Wu, Y. *et al.* A local human Vdelta1 T cell population is associated with survival in nonsmall-cell lung cancer. *Nat Cancer* **3**, 696-709, doi:10.1038/s43018-022-00376-z (2022).

6 de Vries, N. L. *et al.* gammadelta T cells are effectors of immunotherapy in cancers with HLA class I defects. *Nature* **613**, 743-750, doi:10.1038/s41586-022-05593-1 (2023).

7 Rancan, C. *et al.* Exhausted intratumoral Vdelta2(-) gammadelta T cells in human kidney cancer retain effector function. *Nat Immunol* **24**, 612-624, doi:10.1038/s41590-023-01448-7 (2023).

8 Foord, E., Arruda, L. C. M., Gaballa, A., Klynning, C. & Uhlin, M. Characterization of ascites- and tumor-infiltrating gammadelta T cells reveals distinct repertoires and a beneficial role in ovarian cancer. *Sci Transl Med* **13**, doi:10.1126/scitranslmed.abb0192 (2021).

9 Davey, M. S. *et al.* Clonal selection in the human Vdelta1 T cell repertoire indicates gammadelta TCR-dependent adaptive immune surveillance. *Nat Commun* **8**, 14760, doi:10.1038/ncomms14760 (2017).

10 Ravens, S. *et al.* Human gammadelta T cells are quickly reconstituted after stem-cell transplantation and show adaptive clonal expansion in response to viral infection. *Nat Immunol* **18**, 393-401, doi:10.1038/ni.3686 (2017).

11 Willcox, C. R. *et al.* Cytomegalovirus and tumor stress surveillance by binding of a human gammadelta T cell antigen receptor to endothelial protein C receptor. *Nat Immunol* **13**, 872-879, doi:10.1038/ni.2394 (2012).

12 Strid, J. *et al.* Acute upregulation of an NKG2D ligand promotes rapid reorganization of a local immune compartment with pleiotropic effects on carcinogenesis. *Nat Immunol* **9**, 146-154, doi:10.1038/ni1556 (2008).

13 Hayday, A. C. Gammadelta T cells and the lymphoid stress-surveillance response. *Immunity* **31**, 184-196, doi:10.1016/j.immuni.2009.08.006 (2009).

14 Strid, J., Tigelaar, R. E. & Hayday, A. C. Skin immune surveillance by T cells--a new order? *Semin Immunol* **21**, 110-120, doi:10.1016/j.smim.2009.03.002 (2009).

15 Wencker, M. *et al.* Innate-like T cells straddle innate and adaptive immunity by altering antigen-receptor responsiveness. *Nat Immunol* **15**, 80-87, doi:10.1038/ni.2773 (2014).

16 Strid, J., Sobolev, O., Zafirova, B., Polic, B. & Hayday, A. The intraepithelial T cell response to NKG2D-ligands links lymphoid stress surveillance to atopy. *Science* **334**, 1293-1297, doi:10.1126/science.1211250 (2011).

17 Sandrock, I. *et al.* Genetic models reveal origin, persistence and non-redundant functions of IL-17-producing gammadelta T cells. *J Exp Med* **215**, 3006-3018, doi:10.1084/jem.20181439 (2018).

18 Sutton, C. E. *et al.* Interleukin-1 and IL-23 induce innate IL-17 production from gammadelta T cells, amplifying Th17 responses and autoimmunity. *Immunity* **31**, 331-341, doi:10.1016/j.immuni.2009.08.001 (2009).
19 Agerholm, R. & Bekiaris, V. Evolved to protect, designed to destroy: IL-17-producing gammadelta T cells in infection, inflammation, and cancer. *Eur J Immunol* **51**, 2164-2177, doi:10.1002/eji.202049119 (2021).
20 Jandke, A. *et al.* Butyrophilin-like proteins display combinatorial diversity in selecting and maintaining signature intraepithelial gammadelta T cell compartments. *Nat Commun* **11**, 3769, doi:10.1038/s41467-020-17557-y (2020).
21 Di Marco Barros, R. *et al.* Epithelia Use Butyrophilin-like Molecules to Shape Organ-Specific gammadelta T Cell Compartments. *Cell* **167**, 203-218 e217, doi:10.1016/j.cell.2016.08.030 (2016).
22 Turchinovich, G. & Hayday, A. C. Skint-1 identifies a common molecular mechanism for the development of interferon-gamma-secreting versus interleukin-17-secreting gammadelta T cells. *Immunity* **35**, 59-68, doi:10.1016/j.immuni.2011.04.018 (2011).
23 Dart, R. J. *et al.* Conserved gammadelta T cell selection by BTNL proteins limits progression of human inflammatory bowel disease. *Science* **381**, eadh0301, doi:10.1126/science.adh0301 (2023).
24 Bellos, E. *et al.* Heterozygous BTNL8 variants in individuals with multisystem inflammatory syndrome in children (MIS-C). *J Exp Med* **221**, doi:10.1084/jem.20240699 (2024).
25 McKenzie, D. R. *et al.* Normality sensing licenses local T cells for innate-like tissue surveillance. *Nat Immunol* **23**, 411-422, doi:10.1038/s41590-021-01124-8 (2022).
26 Sumaria, N., Grandjean, C. L., Silva-Santos, B. & Pennington, D. J. Strong TCRgammadelta Signaling Prohibits Thymic Development of IL-17A-Secreting gammadelta T Cells. *Cell Rep* **19**, 2469-2476, doi:10.1016/j.celrep.2017.05.071 (2017).
27 Ribot, J. C., Lopes, N. & Silva-Santos, B. gammadelta T cells in tissue physiology and surveillance. *Nat Rev Immunol* **21**, 221-232, doi:10.1038/s41577-020-00452-4 (2021).
28 Hayday, A. C. in *"Gamma delta T cells," in Paul's Fundamental Immunology (Wolters Kluwer/Lippincott Williams & Wikins, 2022)* pp. 1054–1101.
29 Hayday, A. C. *et al.* Structure, organization, and somatic rearrangement of T cell gamma genes. *Cell* **40**, 259-269, doi:10.1016/0092-8674(85)90140-0 (1985).
30 Jones, B., Mjolsness, S., Janeway, C., Jr. & Hayday, A. C. Transcripts of functionally rearranged gamma genes in primary T cells of adult immunocompetent mice. *Nature* **323**, 635-638, doi:10.1038/323635a0 (1986).
31 Jameson, J. M., Cauvi, G., Witherden, D. A. & Havran, W. L. A keratinocyte-responsive gamma delta TCR is necessary for dendritic epidermal T cell activation by damaged keratinocytes and maintenance in the epidermis. *J Immunol* **172**, 3573-3579, doi:10.4049/jimmunol.172.6.3573 (2004).
32 Levelt, C. N. *et al.* Regulation of thymocyte development through CD3: functional dissociation between p56lck and CD3 sigma in early thymic selection. *Immunity* **3**, 215-222, doi:10.1016/1074-7613(95)90091-8 (1995).
33 Carnevale, J. *et al.* RASA2 ablation in T cells boosts antigen sensitivity and long-term function. *Nature* **609**, 174-182, doi:10.1038/s41586-022-05126-w (2022).
34 Lopes, N. *et al.* Distinct metabolic programs established in the thymus control effector functions of gammadelta T cell subsets in tumor microenvironments. *Nat Immunol* **22**, 179-192, doi:10.1038/s41590-020-00848-3 (2021).

35 Pan, Y. *et al.* Survival of tissue-resident memory T cells requires exogenous lipid uptake and metabolism. *Nature* **543**, 252-256, doi:10.1038/nature21379 (2017).
36 Vogel, C. & Marcotte, E. M. Insights into the regulation of protein abundance from proteomic and transcriptomic analyses. *Nat Rev Genet* **13**, 227-232, doi:10.1038/nrg3185 (2012).
37 Fischer, M. A., Jia, L. & Edelblum, K. L. Type I IFN Induces TCR-dependent and -independent Antimicrobial Responses in gammadelta Intraepithelial Lymphocytes. *J Immunol* **213**, 1380-1391, doi:10.4049/jimmunol.2400138 (2024).
38 Ghilas, S. *et al.* Natural killer cells and dendritic epidermal gammadelta T cells orchestrate type 1 conventional DC spatiotemporal repositioning toward CD8(+) T cells. *iScience* **24**, 103059, doi:10.1016/j.isci.2021.103059 (2021).
39 Bottcher, J. P. & Reis e Sousa, C. The Role of Type 1 Conventional Dendritic Cells in Cancer Immunity. *Trends Cancer* **4**, 784-792, doi:10.1016/j.trecan.2018.09.001 (2018).
40 Siddiqui, I. *et al.* Intratumoral Tcf1(+)PD-1(+)CD8(+) T Cells with Stem-like Properties Promote Tumor Control in Response to Vaccination and Checkpoint Blockade Immunotherapy. *Immunity* **50**, 195-211 e110, doi:10.1016/j.immuni.2018.12.021 (2019).
41 Im, S. J. *et al.* Defining CD8+ T cells that provide the proliferative burst after PD-1 therapy. *Nature* **537**, 417-421, doi:10.1038/nature19330 (2016).
42 Spencer, S. P. *et al.* Adaptation of innate lymphoid cells to a micronutrient deficiency promotes type 2 barrier immunity. *Science* **343**, 432-437, doi:10.1126/science.1247606 (2014).
43 Hughes, D. P., Hayday, A., Craft, J. E., Owen, M. J. & Crispe, I. N. T cells with gamma/delta T cell receptors (TCR) of intestinal type are preferentially expanded in TCR-alpha-deficient lpr mice. *J Exp Med* **182**, 233-241, doi:10.1084/jem.182.1.233 (1995).
44 Almeida, A. R. *et al.* Delta One T Cells for Immunotherapy of Chronic Lymphocytic Leukemia: Clinical-Grade Expansion/Differentiation and Preclinical Proof of Concept. *Clin Cancer Res* **22**, 5795-5804, doi:10.1158/1078-0432.CCR-16-0597 (2016).
45 Bravo Garcia-Morato, M. *et al.* New human combined immunodeficiency caused by interferon regulatory factor 4 (IRF4) deficiency inherited by uniparental isodisomy. *J Allergy Clin Immunol* **141**, 1924-1927 e1918, doi:10.1016/j.jaci.2017.12.995 (2018).
46 Moran, A. E. *et al.* T cell receptor signal strength in Treg and iNKT cell development demonstrated by a novel fluorescent reporter mouse. *J Exp Med* **208**, 1279-1289, doi:10.1084/jem.20110308 (2011).
47 Waaler, J. *et al.* Tankyrase inhibition sensitizes melanoma to PD-1 immune checkpoint blockade in syngeneic mouse models. *Commun Biol* **3**, 196, doi:10.1038/s42003-020-0916-2 (2020).
48 Lanca, T. *et al.* Protective role of the inflammatory CCR2/CCL2 chemokine pathway through recruitment of type 1 cytotoxic gammadelta T lymphocytes to tumor beds. *J Immunol* **190**, 6673-6680, doi:10.4049/jimmunol.1300434 (2013).
49 Kao, Y. S. *et al.* Metabolic reprogramming of interleukin-17-producing gammadelta T cells promotes ACC1-mediated de novo lipogenesis under psoriatic conditions. *Nat Metab*, doi:10.1038/s42255-025-01276-z (2025).
50 Myers, D. R., Zikherman, J. & Roose, J. P. Tonic Signals: Why Do Lymphocytes Bother? *Trends Immunol* **38**, 844-857, doi:10.1016/j.it.2017.06.010 (2017).

51 Hartwig, T., Pantelyushin, S., Croxford, A. L., Kulig, P. & Becher, B. Dermal IL-17-producing gammadelta T cells establish long-lived memory in the skin. *Eur J Immunol* **45**, 3022-3033, doi:10.1002/eji.201545883 (2015).
52 Ramirez-Valle, F., Gray, E. E. & Cyster, J. G. Inflammation induces dermal Vgamma4+ gammadeltaT17 memory-like cells that travel to distant skin and accelerate secondary IL-17-driven responses. *Proc Natl Acad Sci U S A* **112**, 8046-8051, doi:10.1073/pnas.1508990112 (2015).
53 Frascoli, M. *et al.* Skin gammadelta T cell inflammatory responses are hardwired in the thymus by oxysterol sensing via GPR183 and calibrated by dietary cholesterol. *Immunity* **56**, 562-575 e566, doi:10.1016/j.immuni.2023.01.025 (2023).
54 Melandri, D. *et al.* The gammadeltaTCR combines innate immunity with adaptive immunity by utilizing spatially distinct regions for agonist selection and antigen responsiveness. *Nat Immunol* **19**, 1352-1365, doi:10.1038/s41590-018-0253-5 (2018).
55 Guo, J. *et al.* gammadelta T cell antigen receptor polyspecificity enables T cell responses to a broad range of immune challenges. *Proc Natl Acad Sci U S A* **121**, e2315592121, doi:10.1073/pnas.2315592121 (2024).
56 Jensen, K. D. *et al.* Thymic selection determines gammadelta T cell effector fate: antigen-naive cells make interleukin-17 and antigen-experienced cells make interferon gamma. *Immunity* **29**, 90-100, doi:10.1016/j.immuni.2008.04.022 (2008).
57 Inacio, D. *et al.* Signature cytokine-associated transcriptome analysis of effector gammadelta T cells identifies subset-specific regulators of peripheral activation. *Nat Immunol* **26**, 497-510, doi:10.1038/s41590-024-02073-8 (2025).
58 Ribot, J. C. *et al.* CD27 is a thymic determinant of the balance between interferon-gamma- and interleukin 17-producing gammadelta T cell subsets. *Nat Immunol* **10**, 427-436, doi:10.1038/ni.1717 (2009).
59 Suzushima, H. *et al.* Discordant gene and surface expression of the T-cell receptor/CD3 complex in adult T-cell leukemia cells. *Cancer Res* **51**, 6084-6088 (1991).
60 Jiang, C. *et al.* Targeting c-Jun inhibits fatty acid oxidation to overcome tamoxifen resistance in estrogen receptor-positive breast cancer. *Cell Death Dis* **14**, 653, doi:10.1038/s41419-023-06181-5 (2023).
61 Hirai, T. *et al.* Keratinocyte-Mediated Activation of the Cytokine TGF-beta Maintains Skin Recirculating Memory CD8(+) T Cells. *Immunity* **50**, 1249-1261 e1245, doi:10.1016/j.immuni.2019.03.002 (2019).

Figures

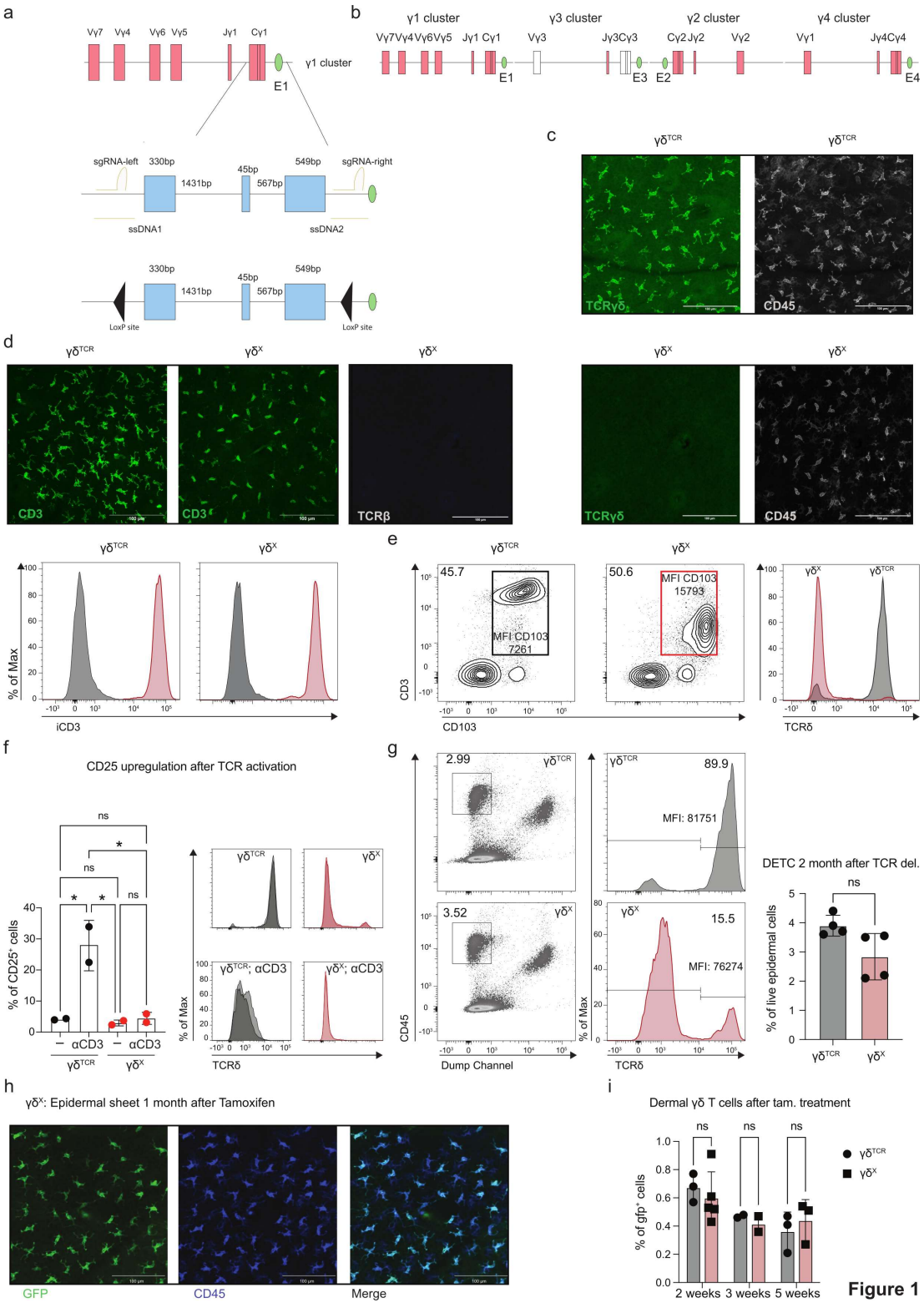


Figure 1

Figure 1

Schematic of the Cγ1 gene cluster and experimental analysis of TCR deletion and γδ T cell dynamics.

(a) The mouse Cγ1 gene cluster, showing Vγ7, Vγ4, Vγ6, Vγ5, Jγ1, and Cγ1 gene segments; sgRNA target sites are indicated, as are LoxP sites [black arrows]; enhancer location (green oval) and exon sizes.

(b) The four mouse TCRγ gene clusters V (variable) and J (junctional) gene segments showing enhancer locations (green ovals). Vg3Jg3Cg3 is shaded white because it is a presumed pseudogene (see text).

(c) Confocal microscopy images of whole-mount ear skin preparations, illustrating TCRγδ (left) CD45 (right) staining in $\gamma\delta^{TCR}$ and $\gamma\delta^{X}$ mice. Scale bars (white) represent 100μm.

(d) Confocal microscopy of whole-mount ear skin preparations stained for CD3 in $\gamma\delta^{TCR}$ and $\gamma\delta^{X}$ mice (top left and centre) and for TCRβ in $\gamma\delta^{X}$ (top right)[scale bars represent 100μm]; lower panels, flow cytometry of intracellular CD3 levels in epidermal $CD45^{+}F4/80^{(neg)}TCRb^{(neg)}CD19^{(neg)}I\text{-}A/I\text{-}E^{(neg)}$ cells in $\gamma\delta^{TCR}$ and $\gamma\delta^{X}$ mice with signal shown in red and isotype control in grey.

(e) Flow cytometry of surface CD3 and CD103 expression on live epidermal single cell suspensions from $\gamma\delta^{TCR}$ and $\gamma\delta^{X}$ mice (representative dot plots (left); TCRδ protein expression on gated cells shown in righthand plots ($\gamma\delta^{TCR}$ mice, grey; $\gamma\delta^{X}$ mice, red).

(f) CD25 expression following overnight culture with or without plate-bound anti-CD3 (bar graphs, (left) and TCRd expression (right) on cells unstimulated (upper), or αCD3 αCD3-stimulated (lower); $\gamma\delta^{TCR}$ mice, grey; $\gamma\delta^{X}$ mice, red.

(g) Left panels: representative gating of $CD45^{+}F4/80^{(neg)}TCRb^{(neg)}CD19^{(neg)}I\text{-}A/I\text{-}E^{(neg)}$ epidermal cells (dump channel) from $\gamma\delta^{TCR}$ and $\gamma\delta^{X}$ mice. Middle panels: Surface TCRδ expression for the gated $CD45^{+}$Dump $Channel^{(neg)}$ cells, with percentages of $TCR\delta^{+}$ cells and gMFI indicated. Right panel: DETC quantification as a percentage of live $CD45^{+}$Dump $Channel^{(neg)}$ cells in $\gamma\delta^{TCR}$ (n=4) (grey) and $\gamma\delta^{X}$ (n=4) mice (red).

(h) Confocal microscopy of whole-mount ear skin preparations showing gfp and CD45 expression and merged images, in $\gamma\delta^{X}$ mice homozygous for Rosa26.mTmG, 4 weeks after tamoxifen treatment (scale bars represent 100μm).

(i) Quantification of gfp^{+} dermal $CD45^{+}$ cells over 2–5 weeks following cre activation by tamoxifen treatment in $\gamma\delta^{TCR}$ and $\gamma\delta^{X}$ mice homozygous for Rosa26.mTmG. Bar graph shows data from $\gamma\delta^{TCR}$ (n=8) (grey) and $\gamma\delta^{X}$ (n=10)(red) mice.

Data pooled from at least two independent experiments. Dots represent individual mice; bars represent mean ± sd. Statistical significance assessed using unpaired two-tailed t-tests: ns, not significant, *P < 0.05.

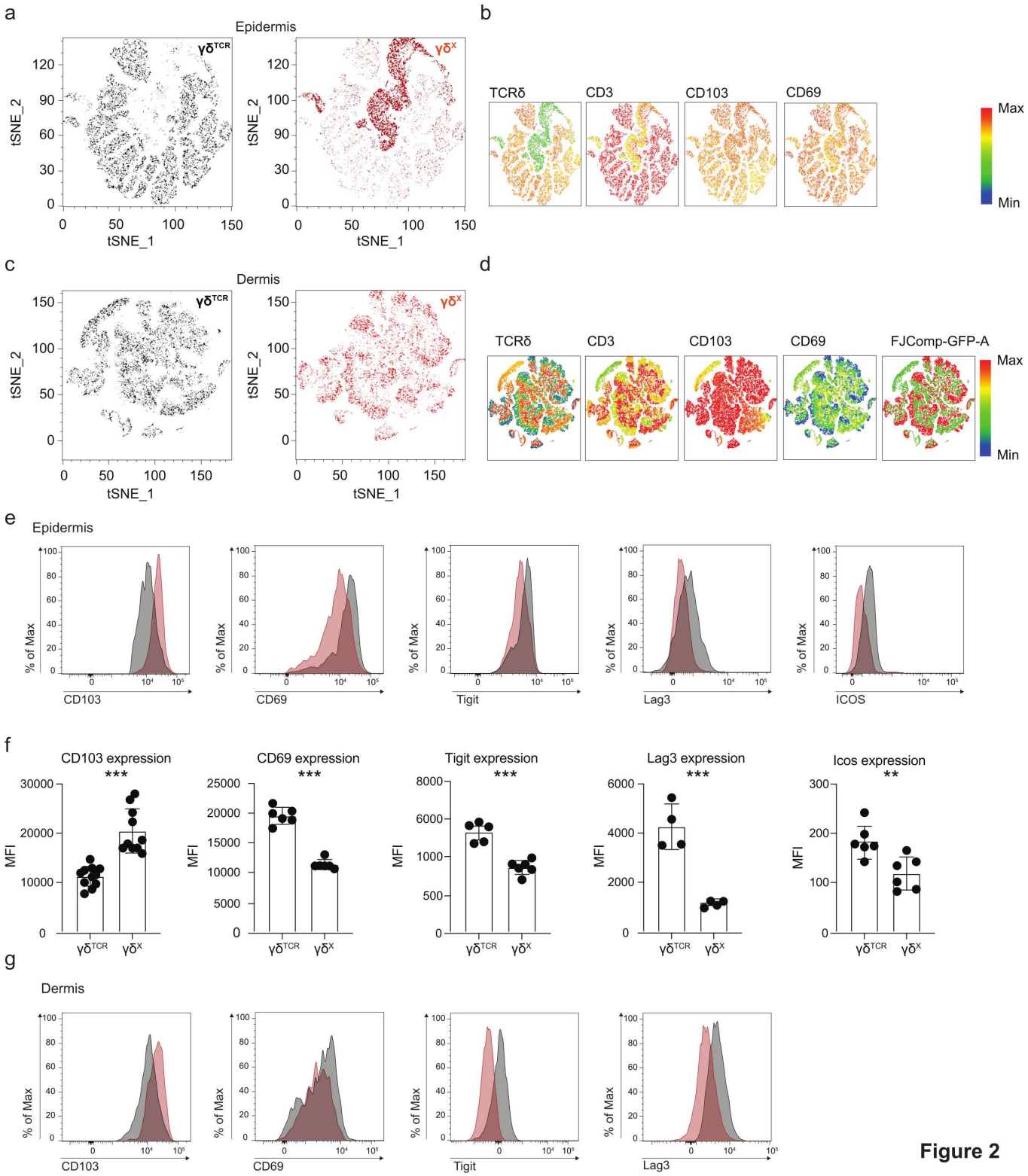


Figure 2

Figure 2

Flow cytometry and t-SNE analysis of epidermal and dermal γδ T cells from γδ^{TCR} and γδ^{X} mice.

(a) t-SNE analysis of epidermal lymphocytes of γδ^{TCR} (grey, n=2) and γδ^{X} (red, n=2) mice. Epidermal CD45^{+}Dump$^{(neg)}$ cells were gated and concatenated for analysis. t-SNE was performed using 10,000 iterations, incorporating all fluorescent parameters except those used for gating, viability and those

directly associated with the TCR (CD3, TCRγδ, and TCRαβ). Samples from $\gamma\delta^{TCR}$ and $\gamma\delta^{X}$ mice were analyzed together in the concatenated dataset but are displayed separately.

(b) Relative expression of markers indicated shown on concatenated t-SNE plots for $\gamma\delta^{TCR}$ and $\gamma\delta^{X}$ cells from (a).

(c) t-SNE analysis of dermal of TCRδ⁺ cells of $\gamma\delta^{TCR}$ mice (grey, n=4) and gfp⁺ cells of $\gamma\delta^{X}$ mice (red, n=5). Cells were gated and concatenated for analysis as in (a), and t-SNE plots determined having excluded those used for gating (TCRd and gfp), viability, CD3, TCRαβ, and tdTomato. Samples were analyzed together in the concatenated dataset but are displayed separately.

(d) Relative expression of markers indicated shown on concatenated t-SNE plots for $\gamma\delta^{TCR}$ and $\gamma\delta^{X}$ cells from (c).

(e) Flow cytometry comparing epidermal $CD45^{+}Dump^{(neg)}$ lymphocytes from $\gamma\delta^{TCR}$ (grey) and $\gamma\delta^{X}$ (red) mice. Representative histograms for indicated marker expression.

(f) Quantification of expression (MFI) for markers as shown in (e) in $CD45^{+}Dump^{(neg)}$ lymphocytes from $\gamma\delta^{TCR}$ and $\gamma\delta^{X}$ mice.

(g) Flow cytometry comparing dermal $TCRd^{+}$ lymphocytes from $\gamma\delta^{TCR}$ (grey) and gfp^{+} lymphocytes from $\gamma\delta^{X}$ (red) mice. Representative histograms for indicated marker expression.

Data pooled from at least two independent experiments. Dots represent individual mice; bars represent mean ± sd. Statistical significance assessed using unpaired two-tailed t-tests: ***P < 0.001, **P < 0.01.

Figure 3

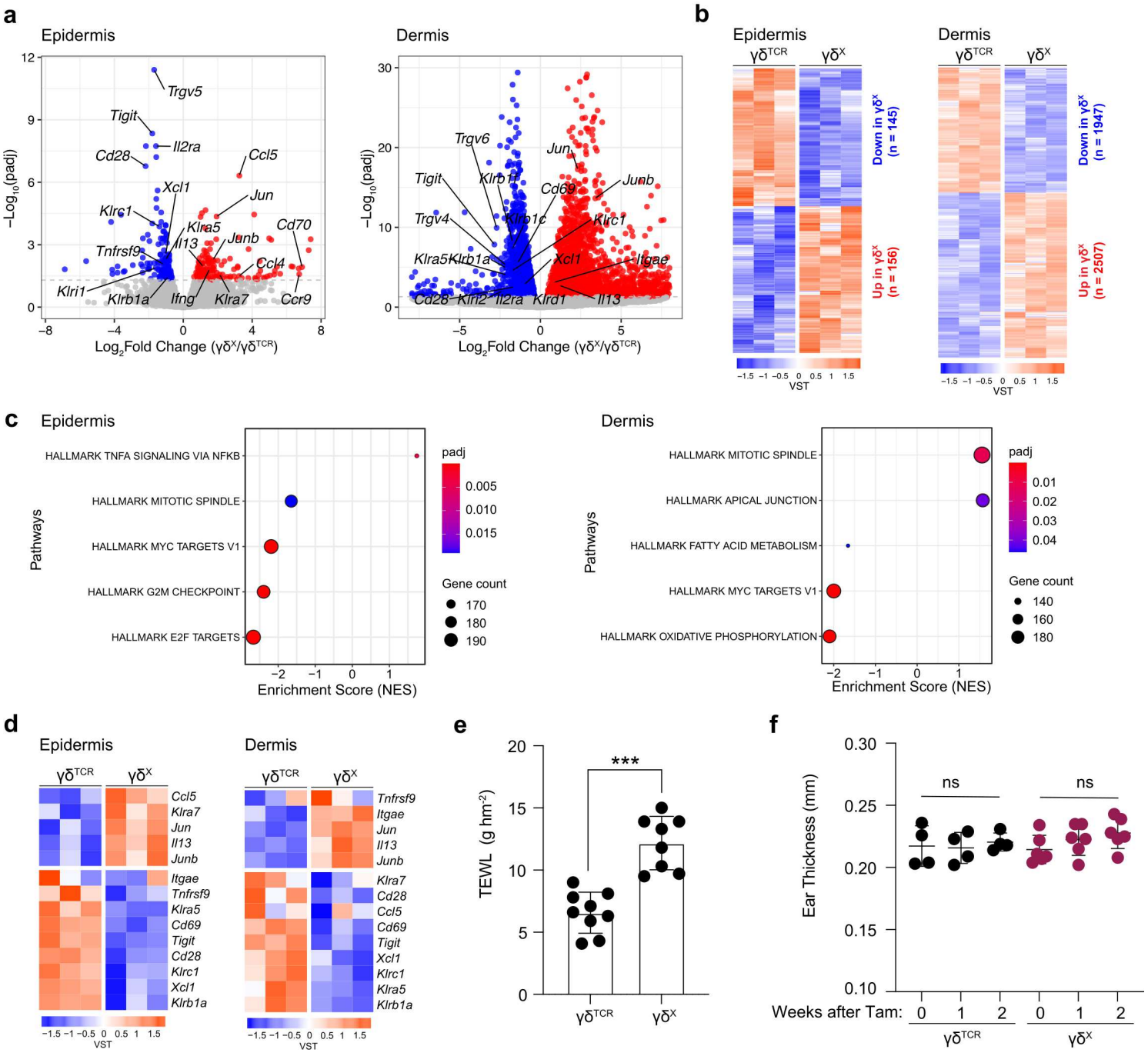


Figure 3

Transcriptional and functional differences in epidermal and dermal lymphocytes from γδ^{TCR} and γδ^{X} mice.

(a) Differential gene expression analysis from RNA-seq in epidermal CD45^{+}Dump$^{(neg)}$ lymphocytes (left) and dermal gfp^{+} lymphocytes (right) isolated from γδ^{X} and γδ^{TCR} mice (n = 3 per group). Volcano plots show significant differentially expressed genes that are downregulated (blue) and upregulated (red) in γδ^{X} cells.

(b) Heatmaps showing significant differentially expressed genes (adjusted *p*-value < 0.05) in epidermal $CD45^{+}Dump^{(neg)}$ lymphocytes (left) and dermal gfp^{+} lymphocytes (right) of $\gamma\delta^{TCR}$ and $\gamma\delta^{X}$ mice. RNA-seq data transcript counts were normalized through variance-stabilized transformation (VST). Numbers of genes downregulated in $\gamma\delta^{X}$ mice (blue) versus upregulated genes (red).

(c) Visualization of gene set enrichment analysis (GSEA) results of differentially expressed genes in epidermal (left) and dermal (right) lymphocytes in $\gamma\delta^{X}$ versus $\gamma\delta^{TCR}$ cells. Dot plots show the top 5 significantly enriched gene sets ranked by normalized enrichment score (NES) using the MSigDB Hallmark gene sets. Dot size is proportional to number of genes detected in each gene set while colour represents significance (adjusted p-values indicated by scale).

(d) Heatmaps display VST-normalized values of representative genes in epidermal (left) and dermal (right) lymphocytes from $\gamma\delta^{TCR}$ and $\gamma\delta^{X}$ mice. Genes selected based on their relevance to γδ T cell activation, cytokine signalling, and tissue residency. Colour scale indicates relative expression levels, ranging from low (blue) to high (red).

(e) Transepidermal water loss (TEWL) measured on ear skin from $\gamma\delta^{TCR}$ (n=9) and $\gamma\delta^{X}$ (n=8) mice two weeks after tamoxifen treatment.

(f) Ear thickness measurement in $\gamma\delta^{TCR}$ and $\gamma\delta^{X}$ mice over time (0, 1, and 2 weeks) after tamoxifen treatment.

Data pooled from at least two independent experiments. Dots represent individual mice; bars represent mean ± s.d. Statistical significance assessed using unpaired two-tailed t-tests: ns, not significant, ***P < 0.001.

Figure 4

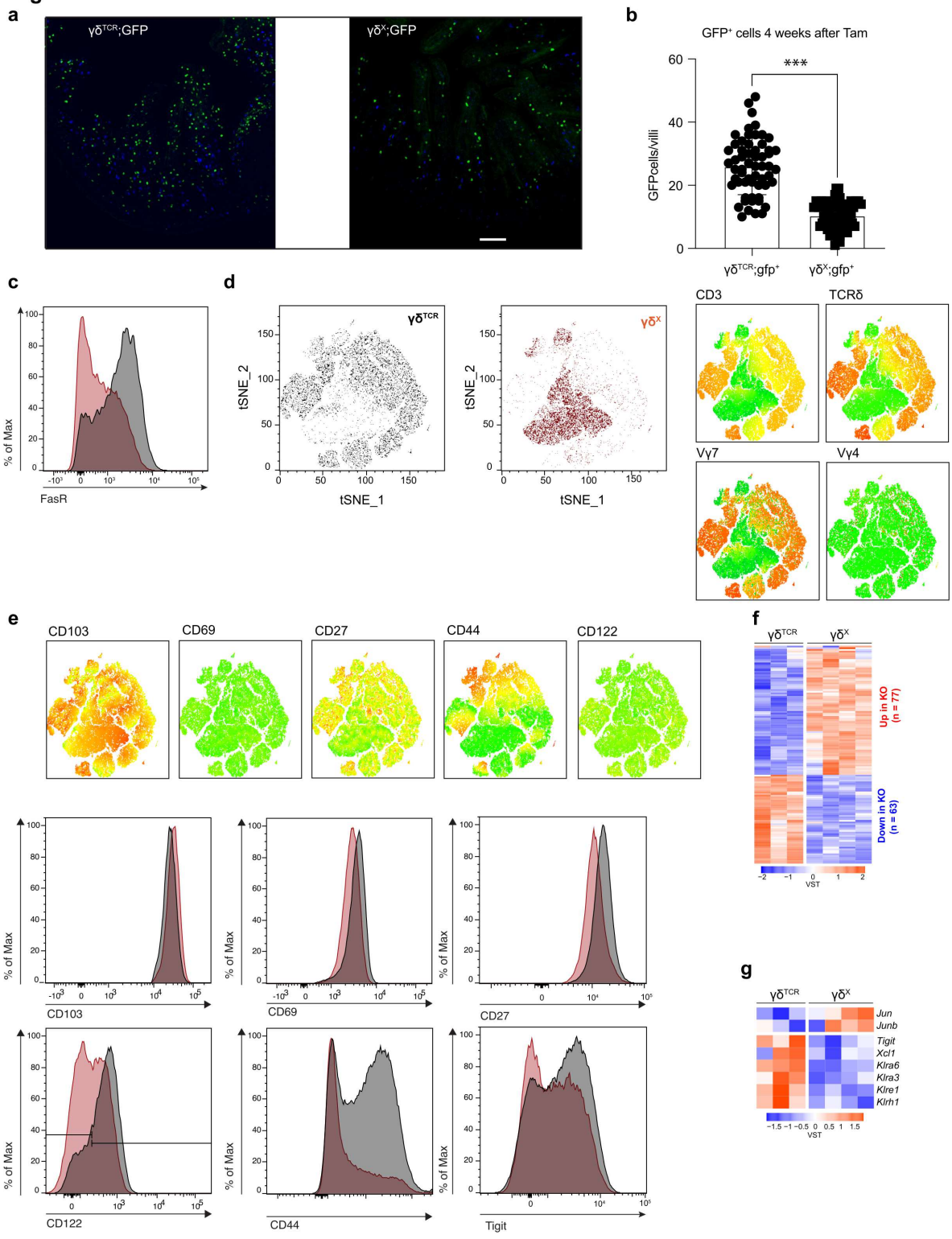


Figure 4

Phenotypic and transcriptonal characterization of intestinal IEL from γδ^{TCR} and γδ^{X} mice.

(a) Confocal microscopy images of distribution of gfp^{+} lymphocytes (green) in the small intestines of mice as indicated. Sections were co-stained for detection of αβ T cells cells (blue). Scale bars represent 100μm. Data are representative images from two independent experiments. For these experiments,

Rosa26.mTmGγδ^{TCR} and Rosa26.mTmGγδ^{X} mice were treated with tamoxifen by oral gavage for 5 consecutive days.

(b) Quantification of gfp^{+} lymphocyte frequencies per villi in frequency in Rosa26.mTmGγδ^{TCR} and Rosa26.mTmGγδ^{X} mice four weeks after tamoxifen treatment. Dots represent one section; bars show mean ± s.d. *** = $p < 0.001$ by unpaired two-tailed t-test.

(c) Representative flow cytometry of FasR surface expression in intestinal IEL of γδ^{TCR} (grey) and γδ^{X} (red) mice.

(d) Spectral flow cytometry of intestinal CD45^{+}Dump$^{(neg)}$ cells. t-SNE analysis was performed (10,000 iterations) including all fluorescent parameters except those markers previously gated, and those for viability and TCR-associated molecules (CD3, TCRγδ, TCRαβ, Vγ7, and Vγ4). γδ^{TCR} (grey, n=3) and γδ^{X} (red, n=3) samples were analysed together and visualized separately (left). t-SNE plots of intestinal IEL displaying expression of CD3, TCRδ, Vγ7, and Vγ4 (right).

(e) Concatenated t-SNE plots of γδ^{TCR} and γδ^{X} IEL from (d) showing relative marker expression for CD103, CDd69, CDd27, CD44 and CD122 (upper). Lower: conventional flow cytometry analysis comparing intestinal IEL from γδ^{TCR} (black) and γδ^{X} (red) mice for indicated markers.

(f) Heatmap showing significant differentially expressed genes (adjusted *p*-value < 0.05) in intestinal IEL from γδ^{TCR} and γδ^{X} mice (indicated). RNA-seq data transcript counts were normalized through variance-stabilized transformation (VST). Numbers of genes downregulated in γδ^{X} mice are shown in blue and upregulated genes in red.

(g) Heatmap displaying VST normalized transcript expression values for specific genes in intestinal IEL from γδ^{TCR} and γδ^{X} mice (indicated). Genes were selected based on trelevance to γδ T cell activation, cytokine signalling, and tissue residency. Colour scale indicates relative expression levels, ranging from low (blue) to high (red).

Figure 5

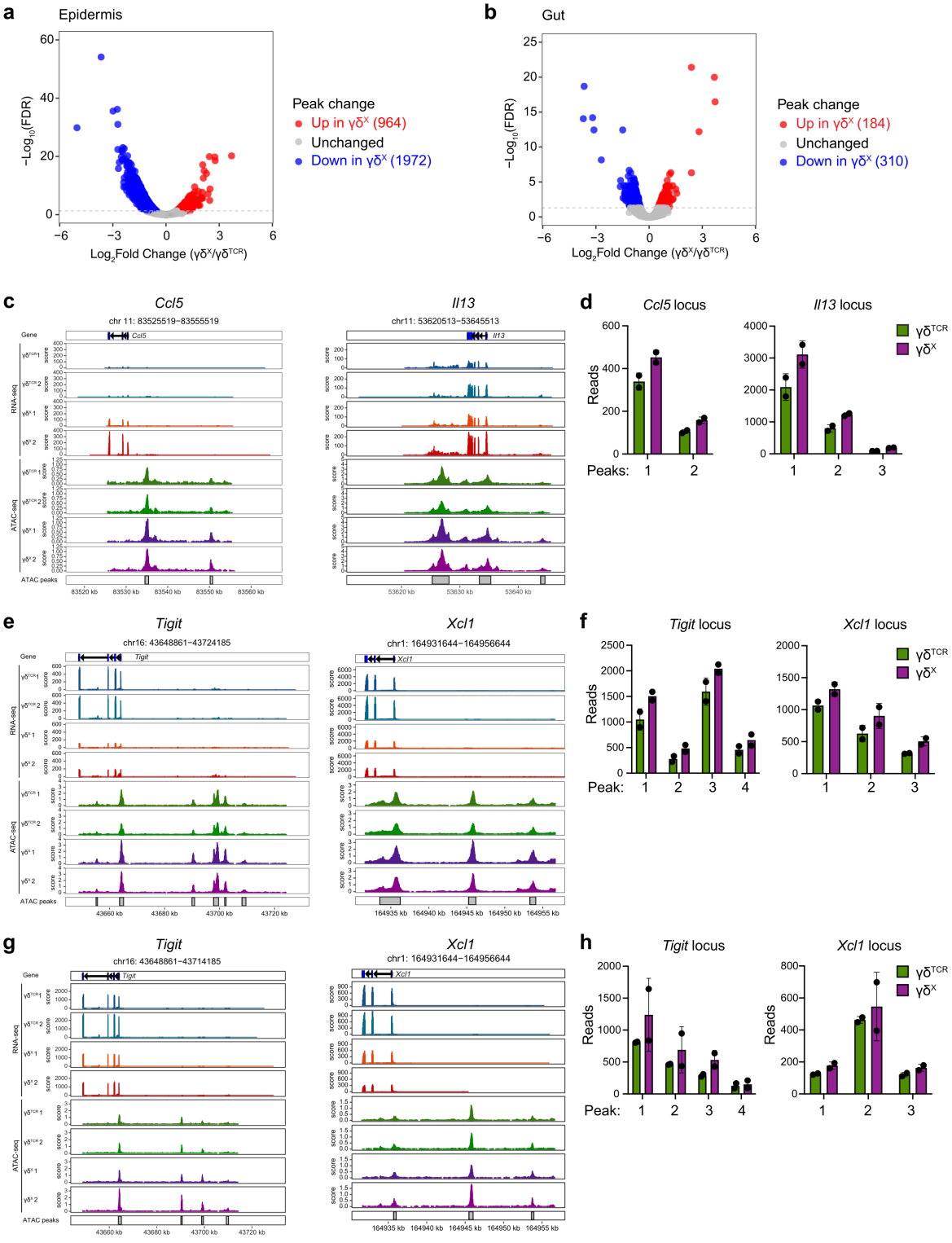


Figure 5

Chromatin accessibility and gene regulation in γδ^{X} versus γδ^{TCR} cells.

(a) Chromatin accessibility analysis performed by ATAC-seq. Volcano plot illustrating genome-wide differential chromatin accessibility between epidermal CD45^{+}Dump$^{(neg)}$ lymphocytes from γδ^{X} and

γδ^{TCR} mice. Numbers of peaks with significant accessibility differences (FDR < 0.05) indicated; increased (red) or decreased (blue) in γδ^{X} cells.

(b) Same as in (a) but for intestinal IEL from γδ^{X} and γδ^{TCR} mice. Numbers of peaks with significant accessibility differences (FDR < 0.05) indicated; increased (red) or decreased (blue) in γδ^{X} cells.

(c, e) Genome browser tracks of ATAC-seq and RNA-seq data showing altered chromatin accessibility and gene expression for *Ccl5* and *Il13 (c), and Tigit and Xcl1* (e) in epidermal, CD45^{+}Dump$^{(neg)}$ γδ^{X} cells compared to CD45^{+}Dump$^{(neg)}$ γδ^{TCR} cells. For each gene locus, RNA-seq tracks (top) and ATAC-seq tracks (bottom) of two paired samples from individual mice were included per genotype. Coordinates are in kb.

(d, f) Quantification of ATAC-seq reads data across different chromatin accessible peaks within selected loci shown in (**c) and (e)**. Each bar represents read counts mean ± s.d. per condition while dots represent individual mice. Peak numbers correspond to different peak positions for each loci starting from the 5' end of the track.

(g) Same as in (e) but in gut IEL from γδ^{X} mice compared to γδ^{TCR} mice.

(h) Same as in (f) but for (g).

Figure 6

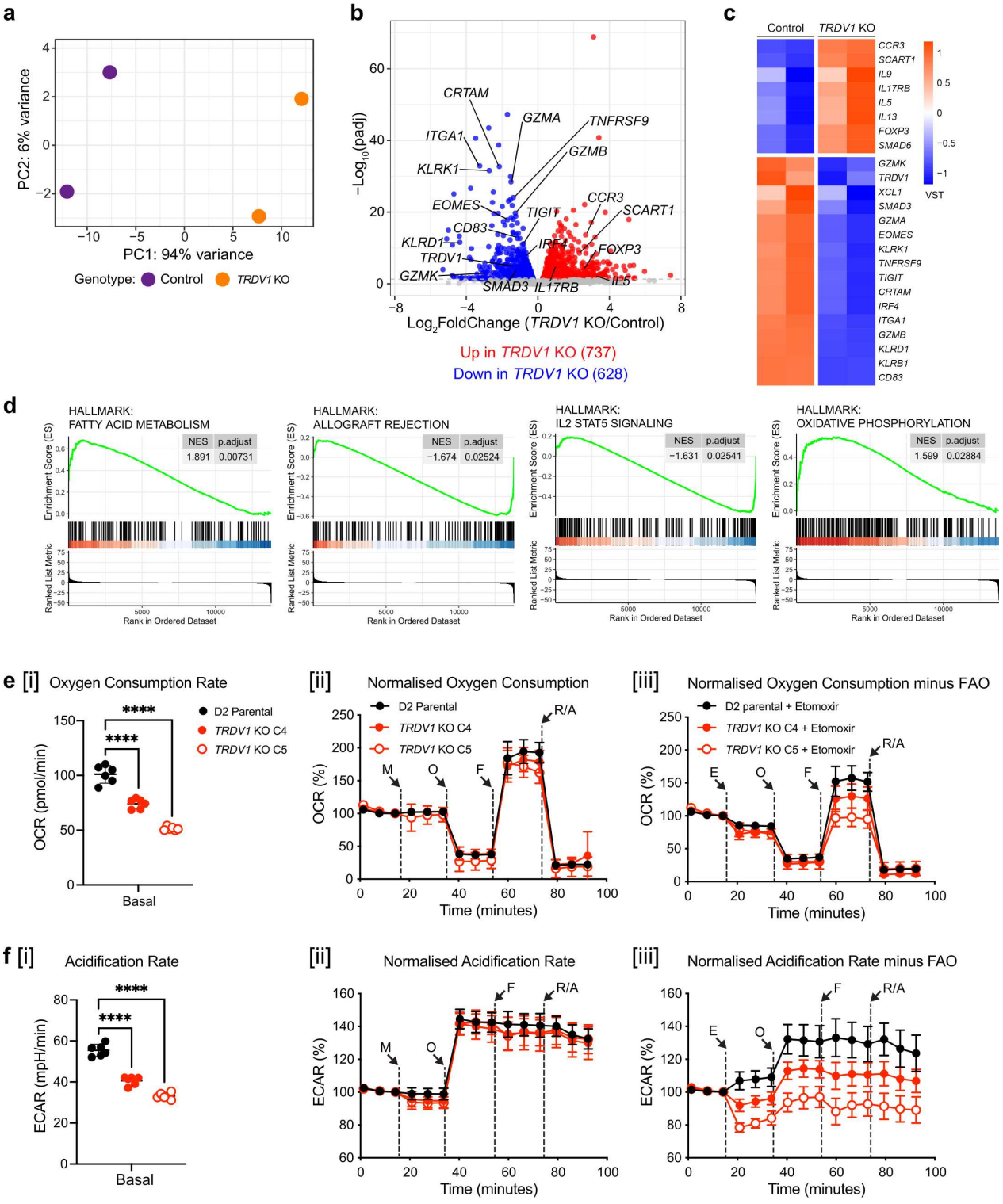


Figure 6

Molecular profiling of human blood-derived HTLV1-immortalised Vδ1$^+$ γδ T cells following *TRDV1* deletion.

(a) Principal component analysis (PCA) of RNA-seq data from HTLV1-immortalised blood-derived control Vδ1$^+$ (**purple**) and *TRDV1* knockout (orange) cells. Percentage variance explained by PC1 and PC2 is

indicated in x and y axis, respectively.

(b) Differential gene expression analysis between *TRDV1* KO and control Vδ1$^+$ cells. Volcano plots show significantly differentially expressed genes (adjusted *p* value < 0.05) downregulated (blue) or upregulated (red) in *TRDV1* KO cells. Selected genes are labelled (n = 2 per genotype). Numbers of DEGs upregulated and downregulated in *TRDV1* KO cells are indicated.

(c) Expression of selected genes in *TRDV1* KO and control Vδ1$^+$ γδ cells. Heatmaps display VST-normalized transcript values. Genes were selected based on relevance to γδ T cell activation, cytokine signalling, and tissue residency (see text). Colour scale indicates relative expression levels, ranging from low (blue) to high (red).

(d) Gene set enrichment analysis (GSEA) results of *TRDV1* KO and control Vδ1$^+$ cells. NES = normalized enrichment score; p.adjust = Benjamini-Hochberg adjusted p value. GSEA plots show the running enrichment score for the top 4 significantly enriched gene sets from Human MSigDB Hallmark gene sets that were ranked based on their NES values. The green line indicates the position of the maximum enrichment score and the black vertical lines show the location of enriched genes in the gene set within the ranked list.

(e) Real-time mitochondrial metabolic profiling of *TRDV1* KO cells (C4 and C5, red and white circles, respectively) compared to parental Vδ1$^+$ cells (D2, black circles) by quantification of oxygen consumption rate (OCR). [i] Basal OCR; [ii] Normalised OCR percentage after sequential injections with oligomycin (after 6th reading), FCCP (after 9th reading) and rotenone together with antimycin A (after 12threading); [iii] Normalised OCR percentage with inhibition of fatty acid oxidation (FAO) by injection with etomoxir (after 3rd reading) prior to sequential injections with oligomycin (after 6th reading), FCCP (after 9threading) and rotenone together with antimycin A (after 12th reading). Vertical dotted lines indicate injection time points with black arrows indicating the injected inhibitor. M: medium only, O: oligomycin, F: FCCP, R/A: rotenone together antimycin A, E: etomoxir.

(f) Same as in (e) but for quantification of extracellular acidification rate (ECAR).

For e and f, each dot marks the mean of 7-9 technical replicate wells for each time point reading per sample. S.D. is also included. Statistical significance assessed using unpaired two-tailed t-tests: **** = P < 0.0001.

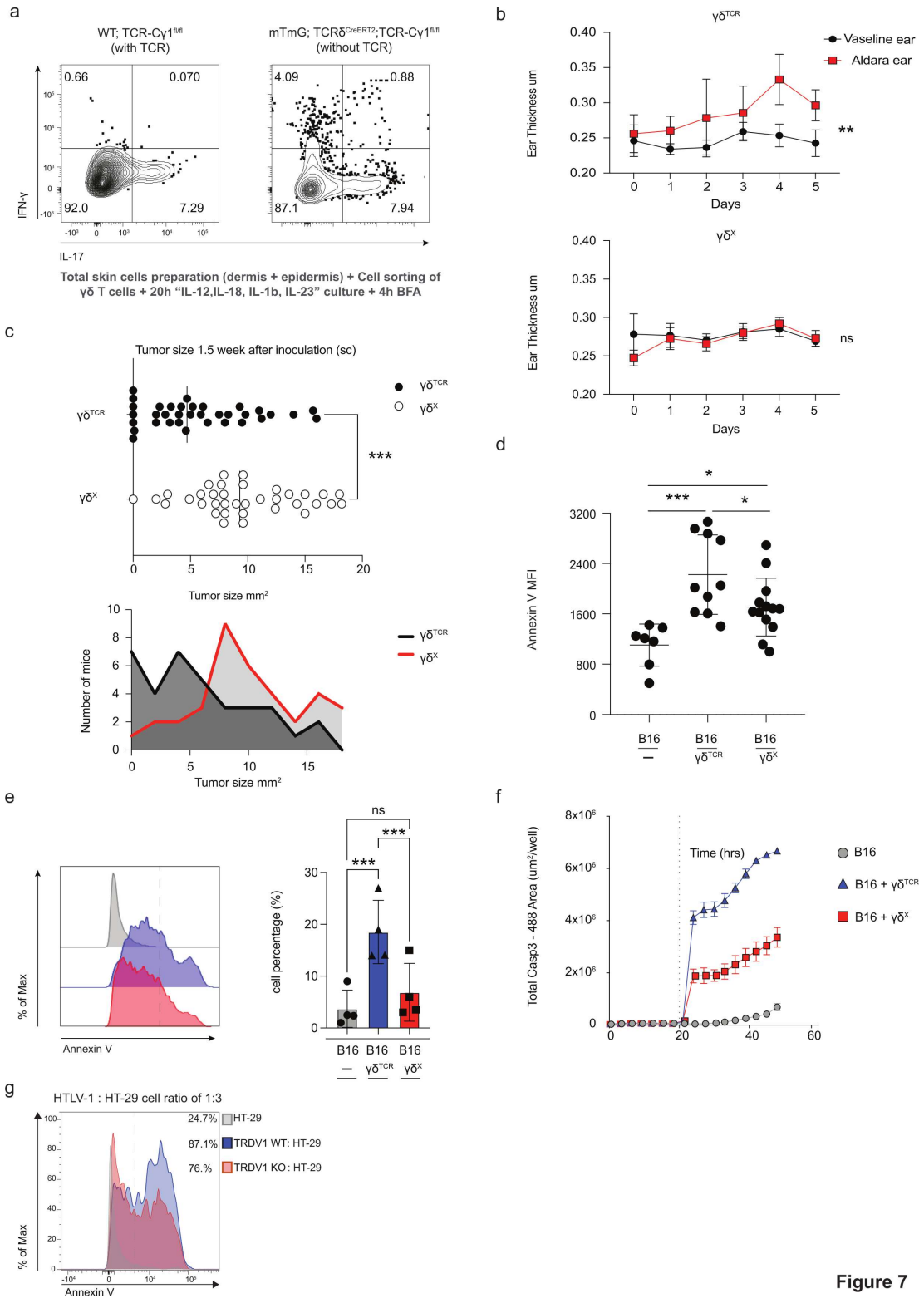


Figure 7

Figure 7

Functional impacts of γδ TCR deletion following challenges

(a) Intracellular cytokine production (IL-17 and IFNγ) by sorted skin CD45^{+}Dump$^{(neg)}$ lymphocytes from γδ^{TCR} (right) and γδ^{X} (left) mice following ex vivo stimulation with IL-12, IL-18, IL-1β, and IL-23 for 21h, with BFA added for last 4h of culture, as indicated.

(b) Ear thickness monitored daily following Aldara or Vaseline application, starting seven days post-tamoxifen in *Tcrg1*$^{+/+}$TCRδ^{CreERT2} (**γ**d^{TCR}) and *Tcrg1*$^{fl/fl}$TCRδ^{CreERT2} (**γ**d^{x}) mice. Statistical analysis was performed between groups on day 5.

(c) Tumour sizes measured at 1.5 weeks after subcutaneous B16-F10 melanoma cell injection into *Tcrg1*$^{+/+}$TCRδ^{CreERT2} (**γ**d^{TCR}, n= 35) and *Tcrg1*$^{fl/fl}$TCRδ^{CreERT2} (**γ**d^{x} n=36) mice, starting seven days post-tamoxifen. Upper panel shows individual tumour sizes per mouse; lower panel depicts tumour size distribution across cohorts.

(d) Bar charts represent the quantification of apoptosis assays using Annexin V staining on B16-F10 melanoma cells co-cultured in vitro at a 1:3 target : effector ratio with cells derived following tamoxifen administration to *Tcrg1*$^{+/+}$TCRδ^{CreERT2} (**γ**d^{TCR}) and *Tcrg1*$^{fl/fl}$TCRδ^{CreERT2} (**γ**d^{x}) mice. Dots represent individual mice.

(e) Representative flow cytometry (left) of Annexin V staining of B16-F10 melanoma cells co-cultured in vitro at a 1:3 target : effector ratio with cells derived following tamoxifen administration to *Tcrg1*$^{+/+}$TCRδ^{CreERT2} (**γ**d^{TCR}) and *Tcrg1*$^{fl/fl}$TCRδ^{CreERT2} (**γ**d^{x}) mice. The dashed vertical line on the histogram represents annexin positivity, which was then quantified in the adjacent graph (right). Dots represent individual mice. TCR in γδ^{X} was deleted in vitro with 4OH-tamoxifen in short-term cultured cells.

(f) Quantification of killing of NucLightRed-transduced B16 cells by γδ T cells in the presence of a green fluorescent caspase-3 reagent, following co-culture in vitro with γδ T cells. Cancer cell apoptosis is measured as total Casp3 - 488 Area (μm²/well).

(g) Representative flow cytometry of Annexin V staining of HT-29 colon carcinoma cells after co-culture with *TRDV1* knockout versus Control γδ cells at 1:3 target: effector ratios. The dashed vertical line on the histogram represents annexin positivity, which was quantified with numbers given in the upper right.

Data are pooled from at least two independent experiments. Dots represent individual mice; bars represent mean ± sd. Statistical significance was assessed using unpaired two-tailed t-tests: ns, not significant; ***P < 0.001, **P < 0.01, *P < 0.05.

Supplementary Files

This is a list of supplementary files associated with this preprint. Click to download.

- SupplementaryTable1v2.docx
- SupplementaryTable2v2.docx
- Figurelegendsv929051700.docx
- SuppFig1.pdf

- SuppFig1v2.pdf
- SuppFig2.pdf
- SuppFig3v2.pdf
- SuppFig4v2.pdf
- SuppFig5v2.pdf
- SuppFig6.pdf
- SuppFig7V2.pdf
- MXMv4.docx